Highlights

Sensitivity Estimation of Stochastic Output with respect to Distribution Parameters of Stochastic Inputs

Xuan-Yi Zhang, Yan-Gang Zhao, Marcos A. Valdebenito, Matthias G.R. Faes

- Sensitivity indices focus on input distribution parameters, not inputs themselves.
- Moments and CDFs of outputs considered, offering exceedance probabilities too.
- Explicit formulas for sensitivity indices derived using moments.
- A dimensional reduction method is implemented for computing moments and parameters.

Sensitivity Estimation of Stochastic Output with respect to Distribution Parameters of Stochastic Inputs

Xuan-Yi Zhang[a,b,*], Yan-Gang Zhao[a], Marcos A. Valdebenito[b], Matthias G.R. Faes[b,c]

[a] *National Key Laboratory of Bridge Safety and Resilience, Beijing University of Technology, Beijing 100124, China*

[b] *Chair for Reliability Engineering, TU Dortmund University, Leonhard-Euler-Str. 5, Dortmund 44227, Germany*

[c] *International Joint Research Center for Engineering Reliability and Stochastic Mechanics, Tongji University, Shanghai 200092, China*

Abstract

Computational models have become indispensable tools for decision-making across numerous fields. Given the inherent randomness in input variables, the outputs of these models are often stochastic, making sensitivity estimation (SE) essential for understanding how variations in inputs affect stochastic outputs. In practice, the input random variables are described by their distribution parameters. This study introduces an SE method to assess the influence of input distribution parameters on the moments and distributions of outputs. Sensitivity indices (SIs) are defined based on both the first three moments and the cumulative distribution function of the outputs, naturally providing SI for exceeding probabilities. A numerical approach is developed to quantify these SIs as the post processing of uncertainty quantification, employing a moment-based model to approximate the output distribution. Three examples, including nonlinear formula and finite element model, are analyzed to demonstrate the applicability and efficiency of the proposed SE method, highlighting its ability to provide a more comprehensive view of the relationship between input distribution parameters and model outputs.

Keywords: Sensitivity, Stochastic output, Mean, Standard deviation, Skewness

1. Introduction

With the rapid development of computational science and simulation technology, mathematical models have become indispensable tools for decision-making in engineering, science, economics, and policy. In practice, these models often involve random inputs, which lead to stochastic outputs. Understanding how uncertainties in the inputs affect the stochastic behavior of the outputs is essential for reliable modeling and informed decision-making [1].

*E-mail: zhangxuanyi@bjut.edu.cn

A wide spectrum of sensitivity estimation (SE) methods has been developed to investigate the influence of input uncertainties on stochastic outputs. These methods can be broadly categorized into two distinct paradigms based on the subject of the sensitivity analysis: sensitivity with respect to input values versus sensitivity with respect to the distribution parameters of inputs.

The first paradigm, which is the most prevalent, defines sensitivity indices with respect to the values of the input random variables. The variance-based SE method represents the most established framework within this paradigm, where the total variance of the output is decomposed into contributions from individual inputs and their interactions [2, 3]. This framework provides a global measure of how input variability affects output variability. Extensions have connected variance-based and derivative-based methods [4, 5, 6], while variogram-based approaches have been introduced to further bridge local and global perspectives [7]. To improve computational efficiency, surrogate-assisted strategies such as polynomial chaos expansion have been widely adopted [8, 9, 10], and successfully applied in many engineering fields [11, 12, 13, 14]. Despite their popularity, variance-based methods capture only the second-order property of the output, which is insufficient for fully describing the stochastic nature of complex systems. To address this limitation, SE methods incorporating higher moments have been developed [15], offering more detailed characterization of output distributions. A more general class is moment-independent methods [16, 17, 18], which quantify sensitivity by comparing the unconditional distribution of the output with its conditional distributions when one or more inputs are fixed. These methods allow for a comprehensive evaluation of how inputs shape the entire output distribution. Nevertheless, all of these approaches share a common aspect: they define sensitivity indices with respect to input values, rather than with respect to the distribution parameters of the inputs. Since distribution parameters explicitly characterize input uncertainty and may be not known precisely when engineering data are limited [19, 20], neglecting them reduces the practical applicability of these methods. It is theoretically possible to treat these distribution parameters as new random variables and apply the above global sensitivity methods. However, this approach conflates the problem of *sensitivity to parameter values* with that of *second-order uncertainty analysis*, leading to conceptual ambiguity. More critically, it necessitates a computationally prohibitive nested framework, making it impractical for most engineering applications.

The second paradigm directly addresses distribution parameters, but has been largely confined to reliability analysis. Here, sensitivity indices (SIs) are defined with respect to the failure prob-

ability or the reliability index. Within the frameworks of first order reliability method (FORM) and second order reliability method (SORM), sensitivities can be obtained analytically in connection with the design point [21, 22]. These approaches are highly efficient when the model is not strongly nonlinear in the Gaussian space and has relatively low dimensionality. Simulation-based reliability methods, including crude Monte Carlo Simulation [23], Importance Sampling [24], Line Sampling [25], and Subset Simulation [26, 27], provide broader applicability and the possibility of reusing samples for sensitivity analysis. To alleviate computational cost, surrogate-assisted reliability methods such as Kriging have been widely explored [28, 29, 30]. In particular, the method of moments (MoM) has demonstrated good efficiency and accuracy for nonlinear systems and rare-event problems [31], and corresponding SE formulations have been proposed [32, 33]. However, reliability-based methods focus only on a single point of the output distribution, typically the cumulative distribution function at a certain threshold, while the remainder of the stochastic output is ignored. Consequently, although input distribution parameters are considered, the full stochastic behavior of the output remains uncharacterized. Crucially, none of these existing methods provides a systematic framework for quantifying the sensitivity of the first three moments (mean, variance, and skewness) of the output distribution to the distribution parameters of the inputs, which is essential for a complete understanding of how input uncertainties shape the central tendency, dispersion, and asymmetry of the output.

In conclusion, existing SE methods either (i) analyze the distribution of outputs but restrict attention to variations in input values, thereby overlooking the role of input distribution parameters, or (ii) incorporate distribution parameters but reduce the output distribution to a single reliability measure. In particular, the sensitivity of the output's moments to these parameters has been largely unexplored. This highlights a critical gap in current methodologies: the lack of SE approaches that systematically quantify how input distribution parameters influence the entire output distribution, including its key moment characteristics, which is essential for comprehensive uncertainty management in engineering practice.

To address this limitation, this study develops a novel SE method that quantifies the sensitivity of output distributions with respect to the distribution parameters of inputs. Two SIs are proposed: a local index for the entire output CDF (which generalizes traditional reliability sensitivities and provides results for all thresholds simultaneously), and a global index for the first three central moments of the output (which is, to our knowledge, a novel contribution offering

direct interpretability of how distribution parameters shift, disperse, or skew the output). For computational efficiency, approximate formulas for these indices are derived using a third-moment normal transformation technique, leading to the so-called TMSE method. In addition, an efficient numerical implementation is introduced as a post-processing step following general uncertainty propagation. The remainder of this paper is organized as follows. Section 2 defines the problem setting. Section 3 introduces the proposed SIs for moments and distributions. Section 4 presents a moment-based approximation for practical application, while Section 5 develops a numerical method for efficient implementation. Section 6 demonstrates the applicability of the proposed method through three numerical examples. Finally, Section 7 concludes the paper.comm

2. Problem statement

2.1. Stochastic system

A stochastic system defines the physical relationship between the inputs $\mathbf{X}$ and output features $\mathbf{Y}$ as follows:

$$\mathbf{Y} = h(\mathbf{X}), \tag{1}$$

where $\mathbf{Y}$=(Y_1,Y_2,...,Y_m) and $\mathbf{X}$=(X_1,X_2,...,X_n) are the vectors of outputs and inputs for the system; m and n are respectively the dimensions of outputs and inputs; and $h(\cdot)$ is the simulator, which builds the mapping from $\mathbf{X}$ to $\mathbf{Y}$ and is usually represented as either a sophisticated code package (e.g., finite element model) or a mathematical function (e.g., performance function).

The uncertainties of the system are first characterized by inputs, and then propagate through the simulator into outputs as shown in Fig. 1. According to the involvements of aleatory or/and

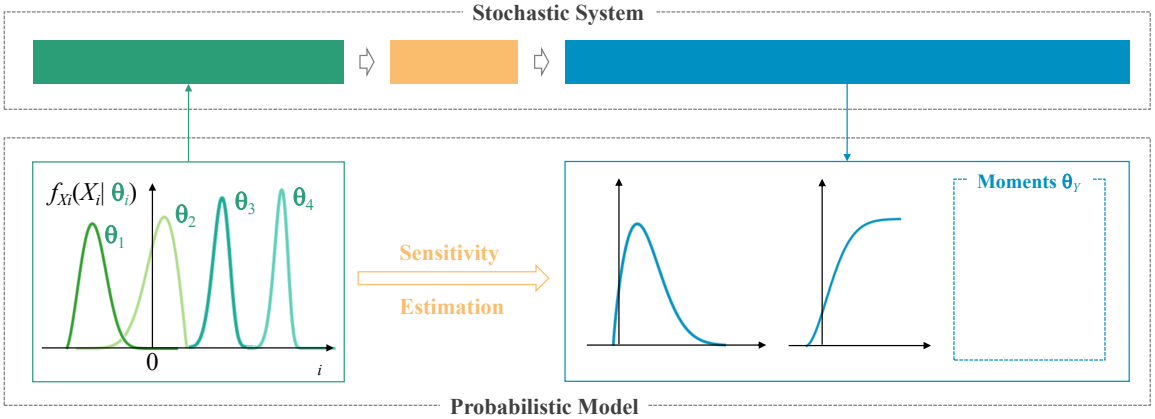

Figure 1: Schematic graph of uncertainty propagation in stochastic system

epistemic uncertainties, components of $\mathbf{X}$ and $\mathbf{Y}$ may be either explicit constants, random variables with fully determined uncertainty characteristics, uncertain constants, or random variables with only vaguely determined uncertain characteristics [34]. In this study, the case when only aleatory uncertainties involved in system parameters are considered, and the uncertain components of $\mathbf{X}$ are modeled as independent random variables with deterministic distribution parameters. For convenience, a single stochastic output of the system, denoted by Y, is investigated in the following, while the results can be extended to multiple outputs.

2.2. Probabilistic model

From the probabilistic perspective, the inputs and outputs of a stochastic system are the probabilistic models of $\mathbf{X}$ and Y. With $\mathbf{X}$ modeled by independent random variables, Y is also a random variable, whose probabilistic models will be discussed in this section.

2.2.1. Probability distribution

The distribution of Y can be described by its cumulative distribution function (CDF) or probabilistic density function (PDF). Based on Eq. (1), the CDF of Y can be computed as follows:

$$F_Y(y, \boldsymbol{\theta}_{\mathbf{X}}) = \int_{\Omega_{\mathbf{X}}} I(\mathbf{x}, y) f_{\mathbf{X}}(\mathbf{x}|\boldsymbol{\theta}_{\mathbf{X}}) d\mathbf{x}, \tag{2}$$

where $F_Y(y, \boldsymbol{\theta}_{\mathbf{X}})$ is the CDF of model output at $Y{=}y$; y is a real value; $\boldsymbol{\theta}_{\mathbf{X}}{=}(\boldsymbol{\theta}_{X_1}, \boldsymbol{\theta}_{X_2},...,\boldsymbol{\theta}_{X_n})$ is the vector of distribution parameters of $\mathbf{X}$, $\boldsymbol{\theta}_{X_i} = (\theta_{i1}, ..., \theta_{ij}, ..., \theta_{in_{X_i}})$ is the vector of distribution parameters of X_i, θ_{ij} is the jth distribution parameter for X_i, and n_{X_i} is the total number of parameters to describe the distribution of X_i; $\Omega_{\mathbf{X}}$ is the domain of $\mathbf{X}$; $I(\cdot, \cdot)$ is the indicator function, which is equal to 1 in case $h(\mathbf{x}) \leq y$ and 0 otherwise; and $f_{\mathbf{X}}(\mathbf{x}|\boldsymbol{\theta}_{\mathbf{X}})$ is the joint PDF of $\mathbf{X}$. Based on Eq. (2), the PDF of Y, denoted by $f_Y(y, \boldsymbol{\theta}_{\mathbf{X}})$, can be computed as follows:

$$f_Y(y, \boldsymbol{\theta}_{\mathbf{X}}) = \frac{\partial F_Y(y, \boldsymbol{\theta}_{\mathbf{X}})}{\partial y}. \tag{3}$$

In general, the CDF is of particular interest for specific value of $Y{=}y$. For instance, when Y represents the load effect, $1 - F_Y(y, \boldsymbol{\theta}_{\mathbf{X}})$ provides the exceeding probability of the load effects for the threshold y. Moreover, if $h(\cdot)$ is defined as the performance function, $F_Y(0, \boldsymbol{\theta}_{\mathbf{X}})$ corresponds to the failure probability. Once the CDF is obtained, the corresponding PDF can be readily

derived based on Eq. (3). Therefore, $F_Y(y, \boldsymbol{\theta}_{\mathbf{X}})$ is the subject of study in the following discussion of sensitivity estimation.

2.2.2. Statistical moments

Central moments of Y are another perspective to describe the stochastic properties of Y, which provide the overall description of the distribution. While incorporating higher-order moments can provide additional information, the computational efficiency decreases significantly as more moments are included. To strike a balance between accuracy and efficiency, the first three central moments of Y are considered, as they capture the majority of the distribution's statistical information [35]. These central moments can be computed from the original moments as follows:

$$\theta_{Y1}(\boldsymbol{\theta}_{\mathbf{X}}) = E_1(\boldsymbol{\theta}_{\mathbf{X}}), \tag{4}$$

$$\theta_{Y2}(\boldsymbol{\theta}_{\mathbf{X}}) = \sqrt{E_2(\boldsymbol{\theta}_{\mathbf{X}}) - [E_1(\boldsymbol{\theta}_{\mathbf{X}})]^2}, \tag{5}$$

$$\theta_{Y3}(\boldsymbol{\theta}_{\mathbf{X}}) = \frac{1}{[\theta_{Y_2}(\boldsymbol{\theta}_{\mathbf{X}})]^3}\{E_3(\boldsymbol{\theta}_{\mathbf{X}}) - 3E_1(\boldsymbol{\theta}_{\mathbf{X}})E_2(\boldsymbol{\theta}_{\mathbf{X}}) + 2[E_1(\boldsymbol{\theta}_{\mathbf{X}})]^3\}, \tag{6}$$

where $\theta_{Y_1}(\boldsymbol{\theta}_{\mathbf{X}})$, $\theta_{Y_2}(\boldsymbol{\theta}_{\mathbf{X}})$, and $\theta_{Y_3}(\boldsymbol{\theta}_{\mathbf{X}})$ are the mean, standard deviation and skewness of Y, respectively; and $E_k(\boldsymbol{\theta}_{\mathbf{X}})$ is the kth moment about the origin of Y and computed from $\boldsymbol{\theta}_{\mathbf{X}}$ as follows:

$$E_k(\boldsymbol{\theta}_{\mathbf{X}}) = \int_{\Omega_{\mathbf{X}}} [h(\mathbf{x})]^k f_{\mathbf{X}}(\mathbf{x}|\boldsymbol{\theta}_{\mathbf{X}}) d\mathbf{x}. \tag{7}$$

3. Derivative-based sensitivity index

As discussed in Eqs. (2)-(7), the probabilistic models of Y are influenced by $\boldsymbol{\theta}_{\mathbf{X}}$. To quantify such influence, the sensitivity of the distribution of Y with respect to $\theta_{X_{ij}}$ (i=1,...,n and j=1,...,n_{X_i}) will be estimated in this section. Without loss of generality, $\boldsymbol{\theta}_{\mathbf{X}}$ can be the the vector of central moments, original moments or other parameters of $\mathbf{X}$, as long as they provide sufficient information to define the distribution of $\mathbf{X}$ unambiguously. Comparison between Eqs. (2) and (7) shows that, $F_Y(y, \boldsymbol{\theta}_{\mathbf{X}})$ provides estimation of the distribution for specific value of Y=y, while the moments are an overall evaluation considering all possible values of Y. In this sense, the sensitivity index (SI) considering $F_Y(y, \boldsymbol{\theta}_{\mathbf{X}})$ is defined as the local SI, while the one considering $\boldsymbol{\theta}_Y$ is named as the global SI. The local and global SIs will be analyzed in this section.

3.1. Local sensitivity index

A straightforward method to quantify the sensitivity output distribution with respect to $\theta_{X_{ij}}$ involves taking the derivatives of the probabilistic models of Y with respect to $\theta_{X_{ij}}$. Then, the local SI of Y with respect to $\theta_{X_{ij}}$, denoted by $LS_{ij}(y, \boldsymbol{\theta}_{\mathbf{X}})$, is defined as follows:

$$LS_{ij}(y, \boldsymbol{\theta}_{\mathbf{X}}) = \frac{\partial F_Y(y, \boldsymbol{\theta}_{\mathbf{X}})}{\partial \theta_{X_{ij}}}. \tag{8}$$

Note that, the local SI defined in Eq. (8) is a function of y and can be interpreted as the SI for the exceedance probability of a threshold b when $y{=}b$.

Substitution of Eq. (2) into Eq. (8) leads to the reformulation of $LS_{ij}(y, \boldsymbol{\theta}_{\mathbf{X}})$ as follows:

$$LS_{ij}(y, \boldsymbol{\theta}_{\mathbf{X}}) = \int_{\Omega}^{\mathbf{x}} I(\mathbf{x}, y) m_{ij}(\mathbf{x}, \boldsymbol{\theta}_{X^i}) f_{\mathbf{X}}(\mathbf{x}|\boldsymbol{\theta}_{\mathbf{X}}) d\mathbf{x}, \tag{9}$$

where $m_{ij}(\mathbf{x}, \boldsymbol{\theta}_{X_i})$ is the so-called score function, which formulated as follows:

$$m_{ij}(\mathbf{x}, \boldsymbol{\theta}_{X_i}) = \frac{\partial f_{\mathbf{X}}(\mathbf{x}|\boldsymbol{\theta}_{\mathbf{X}})}{\partial \theta_{X_{ij}}} \cdot \frac{1}{f\mathbf{x}(\mathbf{x}|\boldsymbol{\theta}\mathbf{x})}. \tag{10}$$

When $\mathbf{X}$ is modeled by independent random variables, $f_{\mathbf{X}}(\mathbf{x}|\boldsymbol{\theta}_{\mathbf{X}})$ is computed as $\prod_{i=1}^{n} f_{X_i}(X_i|\boldsymbol{\theta}_{X_i})$, where $f_{X_i}(X_i|\boldsymbol{\theta}_{X_i})$ is the PDF of X_i. Then, $m_{ij}(\mathbf{x}, \boldsymbol{\theta}_{X_i})$ can be simplified as follows:

$$m_{ij}(\mathbf{x}, \boldsymbol{\theta}_{X_i}) = m_{ij}(x_i, \boldsymbol{\theta}_{X_i}) = \frac{\partial f_{X_i}(x_i|\boldsymbol{\theta}_{X_i})}{\partial \theta_{X_{ij}}} \cdot \frac{1}{f_{X_i}(x_i|\boldsymbol{\theta}_{X_i})}. \tag{11}$$

With the distribution of $\mathbf{X}$ known, $m_{ij}(\mathbf{x}, \boldsymbol{\theta}_{X_i})$ can be readily defined.

3.2. Global sensitivity index

Similarly, the global SI, denoted by $\mathbf{GS}_{ij}(\boldsymbol{\theta}_{\mathbf{X}})$, is proposed as the derivative of central moments of Y with respect to θ_{ij}. As shown in Eqs. (4)-(7), the central moments of Y are computed based on $\boldsymbol{\theta}_{\mathbf{X}}$, and then are represented as a column vector $\boldsymbol{\theta}_Y(\boldsymbol{\theta}_{\mathbf{X}}) = (\theta_{Y1}(\boldsymbol{\theta}_{\mathbf{X}}), \theta_{Y2}(\boldsymbol{\theta}_{\mathbf{X}}), \theta_{Y3}(\boldsymbol{\theta}_{\mathbf{X}}))^T$. Accordingly, $\mathbf{GS}_{ij}(\boldsymbol{\theta}_{\mathbf{X}})$ is formulated as follows:

$$\mathbf{GS}_{ij}(\boldsymbol{\theta}_{\mathbf{X}}) = \frac{\partial \boldsymbol{\theta}_Y(\boldsymbol{\theta}_{\mathbf{X}})}{\partial \theta_{X_{ij}}}. \tag{12}$$

There are three elements in $\mathbf{GS}_{ij}(\boldsymbol{\theta}_{\mathbf{X}})$, corresponding to the mean, standard deviation, and skewness of Y. The second element of $\mathbf{GS}_{ij}(\boldsymbol{\theta}_{\mathbf{X}})$ is analogous to variance-based SIs, except that it

considers the distribution parameters of $\mathbf{X}$ rather than $\mathbf{X}$ itself. Based on Eqs. (4)-(6) and (12), $\mathbf{GS}_{ij}(\boldsymbol{\theta}_{\mathbf{X}})$ can be expanded as follows:

$$\mathbf{GS}_{ij}(\boldsymbol{\theta}_{\mathbf{X}}) = \frac{\partial \boldsymbol{\theta}_Y(\boldsymbol{\theta}_{\mathbf{X}})}{\partial \mathbf{E}(\boldsymbol{\theta}_{\mathbf{X}})} \cdot \frac{\partial \mathbf{E}(\boldsymbol{\theta}_{\mathbf{X}})}{\partial \theta_{X_{ij}}}, \tag{13}$$

where $\mathbf{E}(\boldsymbol{\theta}_{\mathbf{X}}) = (E_1(\boldsymbol{\theta}_{\mathbf{X}}), E_2(\boldsymbol{\theta}_{\mathbf{X}}), E_3(\boldsymbol{\theta}_{\mathbf{X}}))^T$ is a column vector of original moments of Y. Based on Eqs. (4)-(6), $\partial \boldsymbol{\theta}_Y(\boldsymbol{\theta}_{\mathbf{X}})/\partial \mathbf{E}(\boldsymbol{\theta}_{\mathbf{X}})$ is obtained as follows:

$$\frac{\partial \boldsymbol{\theta}_Y(\boldsymbol{\theta}_{\mathbf{X}})}{\partial \mathbf{E}(\boldsymbol{\theta}_{\mathbf{X}})} = \begin{pmatrix} 1 & 0 & 0 \\ -\dfrac{\theta_{Y_1}(\boldsymbol{\theta}_{\mathbf{X}})}{\theta_{Y_2}(\boldsymbol{\theta}_{\mathbf{X}})} & \dfrac{1}{2\theta_{Y_2}(\boldsymbol{\theta}_{\mathbf{X}})} & 0 \\ \dfrac{3\{E_1(\boldsymbol{\theta}_{\mathbf{X}})E_3(\boldsymbol{\theta}_{\mathbf{X}}) - [E_2(\boldsymbol{\theta}_{\mathbf{X}})]^2\}}{[\theta_{Y_2}(\boldsymbol{\theta}_{\mathbf{X}})]^5} & \dfrac{3[E_1(\boldsymbol{\theta}_{\mathbf{X}})E_2(\boldsymbol{\theta}_{\mathbf{X}}) - E_3(\boldsymbol{\theta}_{\mathbf{X}})]}{2[\theta_{Y_2}(\boldsymbol{\theta}_{\mathbf{X}})]^5} & \dfrac{1}{[\theta_{Y_2}(\boldsymbol{\theta}_{\mathbf{X}})]^3} \end{pmatrix}. \tag{14}$$

Based on Eq. (14), $\partial \boldsymbol{\theta}_Y(\boldsymbol{\theta}_{\mathbf{X}})/\partial \mathbf{E}(\boldsymbol{\theta}_{\mathbf{X}})$ can be explicitly computed given the value of $\mathbf{E}(\boldsymbol{\theta}_{\mathbf{X}})$. With first three moments considered, there are three elements in $\partial \mathbf{E}(\boldsymbol{\theta}_{\mathbf{X}})/\partial \theta_{X_{ij}}$ and expressed as follows:

$$\frac{\partial \mathbf{E}(\boldsymbol{\theta}_{\mathbf{X}})}{\partial \theta_{X_{ij}}} = \left(\frac{\partial E_1(\boldsymbol{\theta}_{\mathbf{X}})}{\partial \theta_{X_{ij}}}, \quad \frac{\partial E_2(\boldsymbol{\theta}_{\mathbf{X}})}{\partial \theta_{X_{ij}}}, \quad \frac{\partial E_3(\boldsymbol{\theta}_{\mathbf{X}})}{\partial \theta_{X_{ij}}} \right)^T. \tag{15}$$

Based on Eq. (7), $\partial E_k(\boldsymbol{\theta}_{\mathbf{X}})/\partial \theta_{X_{ij}}$ (k=1, 2, 3) can be computed as follows:

$$\frac{\partial E_k(\boldsymbol{\theta}_{\mathbf{X}})}{\partial \theta_{X_{ij}}} = \int_{\Omega_{\mathbf{x}}} g_{ijk}(\mathbf{x}, \boldsymbol{\theta}_{X_i}) f_{\mathbf{X}}(\mathbf{x}|\boldsymbol{\theta}_{\mathbf{X}}) d\mathbf{x}, \tag{16}$$

where $g_{ijk}(\mathbf{x}, \boldsymbol{\theta}_{X_i})$ is formulated as follows:

$$g_{ijk}(\mathbf{x}, \boldsymbol{\theta}_{X_i}) = [h(\mathbf{x})]^k \cdot m_{ij}(x_i, \boldsymbol{\theta}_{X_i}). \tag{17}$$

4. Moment-based distribution models and local sensitivity index

Direct computation of $F_Y(y, \boldsymbol{\theta}_{\mathbf{X}})$ and $LS_{ij}(y, \boldsymbol{\theta}_{\mathbf{X}})$ based on Eqs. (2) and (9) requires to evaluate a multi-dimensional integral of a function that includes the indicator function $I(\mathbf{x}, y)$. Influenced by $I(\mathbf{x}, y)$, this integral is taken over the domain $\{h(\mathbf{x}) \leq y\}$. In certain cases, such as when $h(\cdot)$ is a summation of independent random variables $\mathbf{X}$, the integral domain defined by $I(\mathbf{x}, y)$ can be explicitly defined, allowing the multi-dimensional integral to be solved analytically (details are provided in Appendix A). However, in most practical situations, the function $h(\cdot)$ is complicated, making it impossible to explicitly determine the region where $\{h(\mathbf{x}) \leq y\}$. As a result, the

required integrals for $F_Y(y, \boldsymbol{\theta}_{\mathbf{X}})$ and $LS_{ij}(y, \boldsymbol{\theta}_{\mathbf{X}})$ cannot be computed directly. In contrast, the moments of Y can be directly obtained based on (4)-(7), since the corresponding integrals are defined over the entire domain of $\mathbf{X}$. To address the challenges in constructing $F_Y(y, \boldsymbol{\theta}_{\mathbf{X}})$ and estimating $LS_{ij}(y, \boldsymbol{\theta}_{\mathbf{X}})$, this section discusses a moment-based approximation approach for these two objectives.

4.1. Moment-based CDF and PDF

To take advantage of well-established theories for standard normal distribution, $F_Y(y, \boldsymbol{\theta}_{\mathbf{X}})$ can be defined based on the normal transformation technique as follows [35]:

$$F_Y(y, \boldsymbol{\theta}_{\mathbf{X}}) \cong \Phi[T(y|\boldsymbol{\theta}_Y(\boldsymbol{\theta}_{\mathbf{X}}))], \tag{18}$$

where $\Phi[\cdot]$ is the CDF of standard normal random variable; and $T(y|\boldsymbol{\theta}_Y(\boldsymbol{\theta}_{\mathbf{X}}))$ is the normal transformation function, which is defined based on $\boldsymbol{\theta}_Y(\boldsymbol{\theta}_{\mathbf{X}})$. Based on Eq. (18), $f_Y(y, \boldsymbol{\theta}_{\mathbf{X}})$ can be easily constructed as follows:

$$f_Y(y, \boldsymbol{\theta}_{\mathbf{X}}) \cong \varphi[T(y|\boldsymbol{\theta}_Y(\boldsymbol{\theta}_{\mathbf{X}}))] \frac{\partial T(y|\boldsymbol{\theta}_Y(\boldsymbol{\theta}_{\mathbf{X}}))}{\partial y}, \tag{19}$$

where $\varphi[\cdot]$ is the PDF of standard normal distribution.

Theoretically, Eqs. (18) and (19) can provide an accurate solution to $F_Y(y, \boldsymbol{\theta}_{\mathbf{X}})$ and $f_Y(y, \boldsymbol{\theta}_{\mathbf{X}})$ with the distribution of Y fully defined by $\boldsymbol{\theta}_Y(\boldsymbol{\theta}_{\mathbf{X}})$. For instance, when $h(\cdot)$ is a sum of independent normal random variables, the resulting distribution is also normal, which can be precisely described using the first two moments. However, in practice, the exact distribution of Y is generally unknown, and finite moments alone are insufficient to fully describe it. As a result, the moment-based formulas in Eqs. (18) and (19) serves as approximations of $F_Y(y, \boldsymbol{\theta}_{\mathbf{X}})$ and $f_Y(y, \boldsymbol{\theta}_{\mathbf{X}})$, with its accuracy depending on the statistical information contained in $\boldsymbol{\theta}_Y(\boldsymbol{\theta}_{\mathbf{X}})$. In this study, the first three central moments of Y are used to define $T(y|\boldsymbol{\theta}_Y(\boldsymbol{\theta}_{\mathbf{X}}))$, as they capture most of the relevant statistical information and have been shown to be sufficient in general cases [35]. However, higher moments may be necessary when Y exhibits strong non-Gaussian behavior.

4.2. Moment-based local sensitivity index

Substitution of Eq. (18) into Eq. (8) leads to the reformulation of $LS_{ij}(y, \boldsymbol{\theta}_{\mathbf{X}})$ as follows:

$$LS_{ij}(y, \boldsymbol{\theta}_{\mathbf{X}}) \cong \frac{\partial \Phi[T(y|\boldsymbol{\theta}_Y(\boldsymbol{\theta}_{\mathbf{X}}))]}{\partial \theta_{X_{ij}}}. \tag{20}$$

Applying the chain rule of differentiation, $LS_{ij}(y, \boldsymbol{\theta}_{\mathbf{X}})$ can be computed as follows:

$$LS_{ij}(y, \boldsymbol{\theta}_{\mathbf{X}}) \cong \varphi[T(y|\boldsymbol{\theta}_Y(\boldsymbol{\theta}_{\mathbf{X}}))] \cdot \frac{\partial T(y|\boldsymbol{\theta}_Y(\boldsymbol{\theta}_{\mathbf{X}}))}{\partial \boldsymbol{\theta}_Y(\boldsymbol{\theta}_{\mathbf{X}})} \cdot \frac{\partial \boldsymbol{\theta}_Y(\boldsymbol{\theta}_{\mathbf{X}})}{\partial \theta_{X_{ij}}}. \tag{21}$$

Substitution Eq (19) into Eq. (21) allows to formulate $LS_{ij}(y, \boldsymbol{\theta}_{\mathbf{X}})$ as follows:

$$LS_{ij}(y, \boldsymbol{\theta}_{\mathbf{X}}) \cong f_Y(y, \boldsymbol{\theta}_{\mathbf{X}}) \cdot \mathbf{NT}(y, \boldsymbol{\theta}_Y(\boldsymbol{\theta}_{\mathbf{X}})) \cdot \mathbf{GS}_{ij}(\boldsymbol{\theta}_{\mathbf{X}}). \tag{22}$$

where $\mathbf{NT}(y, \boldsymbol{\theta}_Y(\boldsymbol{\theta}_{\mathbf{X}}))$ is a 3 dimensional row vector defined based on the normal transformation $T(y|\boldsymbol{\theta}_Y(\boldsymbol{\theta}_{\mathbf{X}}))$ as follows:

$$\mathbf{NT}(y, \boldsymbol{\theta}_Y(\boldsymbol{\theta}_{\mathbf{X}})) = \frac{\partial y}{\partial T(y|\boldsymbol{\theta}_Y(\boldsymbol{\theta}_{\mathbf{X}}))} \cdot \frac{\partial T(y|\boldsymbol{\theta}_Y(\boldsymbol{\theta}_{\mathbf{X}}))}{\partial \boldsymbol{\theta}_Y(\boldsymbol{\theta}_{\mathbf{X}})}. \tag{23}$$

Comparison between Eqs. (12) and (22) reveals that the local sensitivity index $LS_{ij}(y, \boldsymbol{\theta}_{\mathbf{X}})$ is a function of the global sensitivity index $\mathbf{GS}_{ij}(\boldsymbol{\theta}_{\mathbf{X}})$. This relationship exists because the global SI offers an overall evaluation of the distribution of Y, but lacks the ability to describe specific values. Therefore, $LS_{ij}(y, \boldsymbol{\theta}_{\mathbf{X}})$ provides a more detailed assessment of sensitivity compared to $\mathbf{GS}_{ij}(\boldsymbol{\theta}_{\mathbf{X}})$.

4.3. Third moment normal transformation based approximation

As discussed above, the key task for determining the moment-based $F_Y(y, \boldsymbol{\theta}_{\mathbf{X}})$, $f_Y(y, \boldsymbol{\theta}_{\mathbf{X}})$ and $LS_{ij}(y, \boldsymbol{\theta}_{\mathbf{X}})$ is to define the normal transformation function $T(y|\boldsymbol{\theta}_Y(\boldsymbol{\theta}_{\mathbf{X}}))$. In this study, the third-moment normal transformation (TMNT) is applied [36], which is proved to be efficient while achieving sufficient. For simplicity, in the following, $\boldsymbol{\theta}_Y(\boldsymbol{\theta}_{\mathbf{X}})$ and $\theta_{Y_k}(\boldsymbol{\theta}_{\mathbf{X}})$ and $E_k(\boldsymbol{\theta}_{\mathbf{X}})$ (k=1, 2, 3) will be denoted as $\boldsymbol{\theta}_Y$, θ_{Y_k} and E_k, respectively. Based on the TMNT, $T(y|\boldsymbol{\theta}_Y)$ is approximated as follows:

$$T(y|\boldsymbol{\theta}_Y) \cong \begin{cases} \dfrac{-a_2 + \Delta}{2a_1}, & \theta_{Y_3} \neq 0 \\ y_s, & \theta_{Y_3} = 0 \end{cases} \tag{24}$$

where

$$\Delta = \sqrt{a_2^2 + 4a_1(a_1 + y_s)}, \tag{25}$$

$$y_s = \frac{(y - \theta_{Y_1})}{\theta_{Y_2}}, \tag{26}$$

where y_s is the standardization of y; and a_1 and a_2 are the parameters of the TMNT computed from θ_{Y_3}. The applicable range for the TMNT is given as follows [35]:

$$-120\epsilon_a\theta_{2Y}/\theta_{1Y} \leq \theta_{3Y} \leq 40\epsilon_a\theta_{2Y}/\theta_{1Y}, \tag{27}$$

where ϵ_a is the allowable error. For problem with $|\theta_{Y_3}| \leq 2$, a_1 and a_2 can be calculated as follows [37]:

$$a_1 = \frac{\sqrt{3}}{10}\theta_{Y_3}, \quad a_2 = 1 - \frac{\sqrt{3}}{50}\theta_{Y_3}^2. \tag{28}$$

Based on Eqs. (24)-(28), $\partial T(y|\boldsymbol{\theta}_Y)/\partial y$ can be directly obtained as follows:

$$\frac{\partial T(y|\boldsymbol{\theta}_Y)}{\partial y} \cong \frac{1}{\theta_{Y_2}\Delta}. \tag{29}$$

Substitution Eq. (29) into (19) yields $f_Y(y, \boldsymbol{\theta}_{\mathbf{X}})$:

$$f_Y(y, \boldsymbol{\theta}_{\mathbf{X}}) \cong \frac{\varphi[T(y|\boldsymbol{\theta}_Y)]}{\theta_{Y_2}\Delta}. \tag{30}$$

Based on Eqs. (24)-(28), $\partial T(y|\boldsymbol{\theta}_Y)/\partial \boldsymbol{\theta}_Y$ can be obtained as follows:

$$\frac{\partial T(y|\boldsymbol{\theta}_Y)}{\partial \boldsymbol{\theta}_Y} \cong \left(-\frac{1}{\theta_{Y_2}\Delta}, \quad -\frac{y_s}{\theta_{Y_2}\Delta}, \quad \frac{\partial T(y|\boldsymbol{\theta}_Y)}{\partial \theta_{Y_3}}\right). \tag{31}$$

Combine Eqs. (23), (29) and (31), $\mathbf{NT}(y, \boldsymbol{\theta}_Y)$ can be obtained as follows:

$$\mathbf{NT}(y, \boldsymbol{\theta}_Y) \cong \left(-1, \quad -y_s, \quad NT_3(y, \boldsymbol{\theta}_Y)\right). \tag{32}$$

When $\theta_{Y3} = 0$, $NT_3(y, \boldsymbol{\theta}_Y) = 0$; when $\theta_{Y3} \neq 0$, $NT_3(y, \boldsymbol{\theta}_Y)$ is formulated as follows:

$$NT_3(y, \boldsymbol{\theta}_Y) \cong \frac{\theta_{Y2}}{\theta_{Y3}}\left[(2 - a_2)T(y|\boldsymbol{\theta}_Y) - y_s\right]. \tag{33}$$

As discussed above, both the TMNT and corresponding $\mathbf{NT}(y, \boldsymbol{\theta}_Y)$ can be analytically determined based on the value of $\boldsymbol{\theta}_Y$. Then, based on the TMNT, the moment-based CDF and PDF of Y can be explicitly constructed using Eqs. (18) and (30), respectively. Given the values of PDF of Y, $\mathbf{NT}(y, \boldsymbol{\theta}_Y)$ and global SI, the moment-based local SI can be readily computed using Eq. (22). To sum up, by using the TMNT and the moments of Y, the moment-based CDF and PDF of Y as well as the moment-based local SI can be explicitly computed, with no extra model evaluation required. This helps to improve the computational efficiency. As the sensitivity estimation method with respect to input distribution parameters is developed based on the TMNT, it is referred to as TMSE method.

5. Numerical method for sensitivity estimation

The fundamental step for TMSE method is to evaluate the moments of Y and global SI. Based on Eqs. (4)-(7) and (12)-(13), the moments of Y and global SI can be computed based on multi-dimensional integrals over the domain of $\mathbf{X}$ given in Eqs. (7) and (16). As the dimension of $\mathbf{X}$ is generally large in practice, direct computation of these two integrals may be time-consuming or even impossible. As an alternative, efficient dimensional reduction method for integral approximation is introduced in this section.

5.1. Dimensional reduction method for evaluating the original moments

To make a good balance between accuracy and efficiency, the original moments of Y, i.e., E_k, is solved using the point estimate method [38] combining with bivariate dimensional reduction method (BDRM) [39] as follows:

$$E_k \cong \sum_{1\le p<q\le n} E_{pq}^k - (n-2)\sum_{p=1}^{n} E_p^k + \frac{(n-1)(n-2)}{2}[h(\boldsymbol{\mu})]^k, \tag{34}$$

$$E_{pq}^k = \sum_{r_p=1}^{l}\sum_{r_q=1}^{l} P_{r_p}P_{r_q}h[\mathbf{x}_{pq}(r_p, r_q)]^k, \quad E_p^k = \sum_{r_p=1}^{l} P_{r_p}h[\mathbf{x}_p(r_p)]^k, \tag{35}$$

where $\boldsymbol{\mu}$ is the vector of mean values of $\mathbf{X}$; $\mathbf{x}_{pq}(r_p, r_q)$=($\mu_1$,..., $T^{-1}(\hat{\mathbf{u}}(r_p), \boldsymbol{\theta}_{X_p})$,..., $T^{-1}(\hat{\mathbf{u}}(r_q), \boldsymbol{\theta}_{X_q})$,..., μ_n) and $\mathbf{x}_p(r_p)$ =(μ_1,..., $T^{-1}(\hat{\mathbf{u}}(r_p), \boldsymbol{\theta}_{X_p})$,..., μ_n) are the evaluation points; $T^{-1}(\cdot,\cdot)$ is the inverse normal transformation function, which can be defined using Rosenblatt transformation [40]; $\hat{\mathbf{u}}$ is a l-dimensional vector of the evaluation points in standard normal space; P_{r_p} and P_{r_q} are the r_pth

and r_qth elements in $\hat{\mathbf{P}}$, respectively; and $\hat{\mathbf{P}}$ is the weight vector corresponding to $\hat{\mathbf{u}}$. $\hat{\mathbf{P}}$ and $\hat{\mathbf{u}}$ can be computed as follows [38]:

$$\hat{\mathbf{u}} = \sqrt{2}\boldsymbol{\zeta}, \quad \hat{\mathbf{P}} = \frac{1}{\pi}\boldsymbol{\xi}. \tag{36}$$

where $\boldsymbol{\zeta}$ and $\boldsymbol{\xi}$ are vectors of the abscissa and corresponding weights in the Gauss-Hermite quadrature formula, respectively. Generally, the accuracy of point estimate method can be guaranteed with $l = 7$ [38], and the evaluation points $\hat{\mathbf{u}}$ and corresponding weights $\hat{\mathbf{P}}$ are given as follows [38]:

$$\hat{\mathbf{u}} = (\pm 3.7504, \pm 2.3668, \pm 1.1544, 0), \quad \hat{\mathbf{P}} = (0.0005, 0.0308, 0.2401, 0.4574). \tag{37}$$

Based on Eqs. (34) and (35), the number of model evaluations required for computing $\mathbf{E}$, denoted by N_M, is

$$N_M = \frac{n(n-1)}{2}(l-1)^2 + n(l-1) + 1 \tag{38}$$

It can be seen that N_M is proportional to n^2, which becomes extremely large for high-dimensional problems. Thus, the proposed method may face challenges for large n. This curse of dimensionality arises from the applied dimension-reduction method [39], and it may be alleviated through alternative approximation techniques.

5.2. Dimensional reduction method for estimating global SI

Comparison between Eqs. (7) and (16) reveals that, $\partial E_k/\partial\theta_{X_{ij}}$ can be integrated as the mean value of $g_{ijk}(\mathbf{X}, \boldsymbol{\theta}_{X_i})$. Furthermore, the input random variables for both $h(\cdot)$ and $g_{ijk}(\mathbf{X}, \boldsymbol{\theta}_{X_i})$ are $\mathbf{X}$. Thus, $\partial E_k/\partial\theta_{X_{ij}}$ can be evaluated using the same method as for E_k, i.e., the point estimate method combining with BDRM as follows:

$$\frac{\partial E_k}{\partial \theta_{ij}} \cong \sum_{1\le p<q\le n} D_{pq} - (n-2)\sum_{p=1}^{n} D_p + \frac{(n-1)(n-2)}{2} g_{ijk}(\boldsymbol{\mu}, \boldsymbol{\theta}_{X_i}), \tag{39}$$

$$D_{pq} = \sum_{r_p=1}^{l}\sum_{r_q=1}^{l} P_{r_p} P_{r_q} g_{ijk}[\mathbf{x}_{pq}(r_p, r_q), \boldsymbol{\theta}_{X_i}], \quad D_p = \sum_{r_p=1}^{l} P_{r_p} g_{ijk}[\mathbf{x}_p(r_p), \boldsymbol{\theta}_{X_i}]. \tag{40}$$

Eqs.(34)-(35) and (39)-(40) show that, the evaluation points applied for evaluating $\mathbf{E}$ and $\partial\mathbf{E}/\partial\theta_{X_{ij}}$ are the same. Compared with the estimation of $\mathbf{E}$, the only extra requirements for estimating $\partial\mathbf{E}/\partial\theta_{X_{ij}}$ is to compute $m_{ij}(X_i|\boldsymbol{\theta}_{X_i})$ as given in Eq. (10), which can be easily determined. There is no extra model evaluation required for computing $\partial\mathbf{E}/\partial\theta_{X_{ij}}$, and thus, it can be treated as the

byproduct of determining $\mathbf{E}$, which guarantees the computational efficiency.

5.3. Procedure of the proposed method

The procedure of the proposed TMSE method for sensitivity estimation of distribution of Y with respect to $\theta_{X_{ij}}$ is summarized in Fig. 2, which comprises three main steps as detailed below:

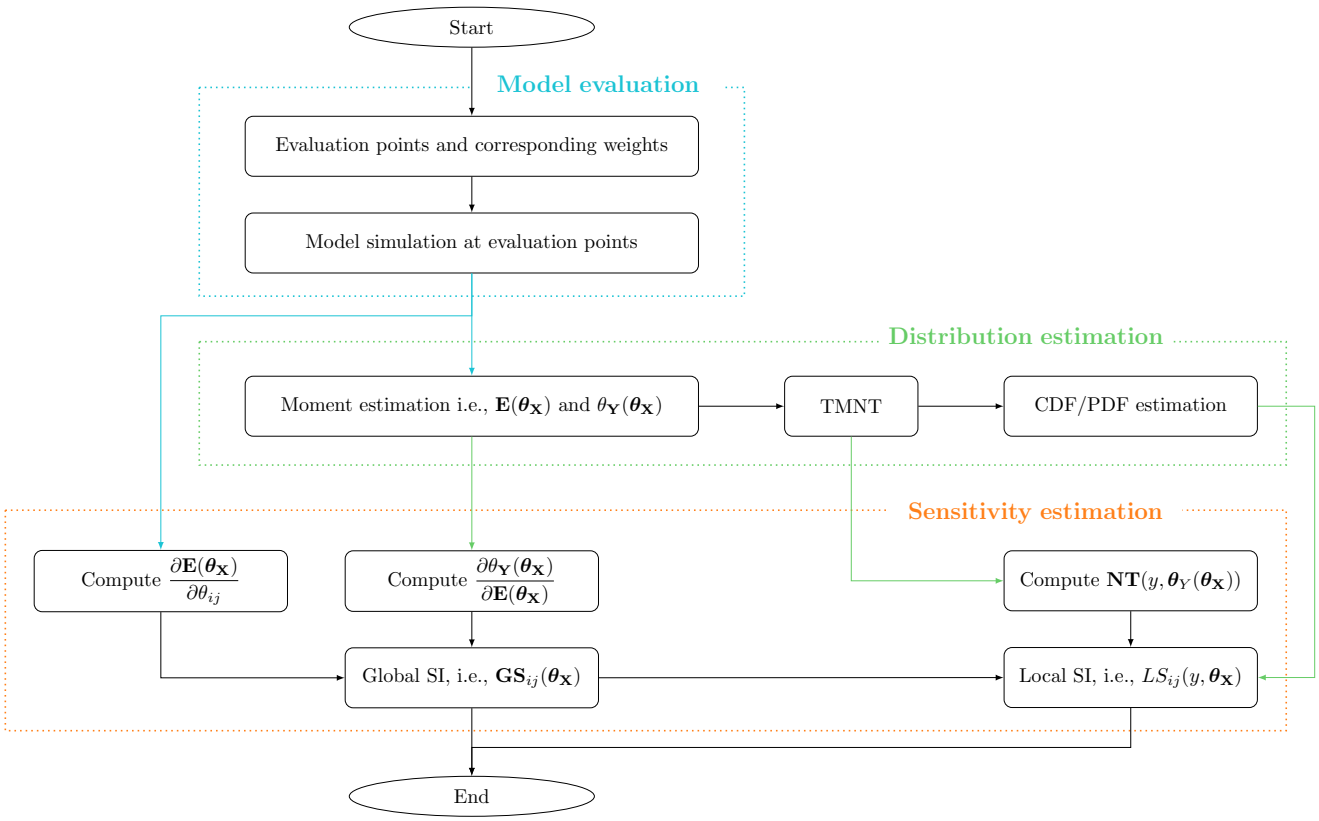

Figure 2: Flowchart for sensitivity estimation of output distribution using the TMSE method

(1) **Model evaluation.**

- *Evaluation points generation.* First, evaluation points for each random variable are transformed from $\hat{\mathbf{u}}$, using inverse normal transformation technique such as Rosenblatt transformation. Then, all $\mathbf{x}_{pq}(r_p, r_q)$ and $\mathbf{x}_p(r_p)$ $(1 \leq p < q \leq n,\ r_p{=}1,...,l$ and $r_q{=}1,..., l)$ are formed with different combinations of the evaluation points.
- *Model evaluation.* With the set of evaluation points, the corresponding values of the output Y are computed using the estimator $h(\cdot)$. It is important to note that this is the only step requiring model evaluation, i.e., evaluating $h(\cdot)$. The values of Y obtained in this step are subsequently used for distribution estimation and are reused in the sensitivity estimation.

(2) **Distribution estimation.**

- *Moment estimation of the output.* Based on the values of Y at the evaluation points and Eqs. (34) and (35), the original moments of Y, i.e., $\mathbf{E}$, can be computed. Then, with the aid of Eq. (4)-(6), the central moments of Y, i.e., $\boldsymbol{\theta}_Y$, can be obtained. The obtained $\mathbf{E}$ and $\boldsymbol{\theta}_Y$ will be applied to both distribution evaluation and sensitivity estimation.
- *CDF and PDF simulation.* Based on $\boldsymbol{\theta}_Y$, the TMNT for y can be constructed using Eqs. (24)-(26). Then, CDF and PDF of Y can be directly constructed using Eqs. (18) and (30), respectively.

(3) **Sensitivity estimation.**

- Estimate $\partial\mathbf{E}/\partial\theta_{X_{ij}}$ using the point estimate point combined with BDRM, as given in Eqs. (39)-(40). The values of $g_{ijk}(\cdot,\cdot)$ at the evaluation points are computed based on the values of Y obtained previously, and thus there is no extra model evaluation required.
- Compute $\partial\boldsymbol{\theta}_Y/\partial\mathbf{E}$. With $\boldsymbol{\theta}_Y$ and $\mathbf{E}$ obtained in distribution evaluation, $\partial\boldsymbol{\theta}_Y/\partial\mathbf{E}$ can be directly computed using Eq. (14).
- Estimate the global SI $\mathbf{GS}_{ij}(\boldsymbol{\theta}_\mathbf{X})$ based on Eq. (13), using the results of $\partial\mathbf{E}(\boldsymbol{\theta}_\mathbf{X})/\partial\theta_{X_{ij}}$ and $\partial\boldsymbol{\theta}_Y(\boldsymbol{\theta}_\mathbf{X})/\partial\mathbf{E}(\boldsymbol{\theta}_\mathbf{X})$.
- Compute $\mathbf{NT}(y,\boldsymbol{\theta}_Y)$. With the TMNT constructed, $\mathbf{NT}(y,\boldsymbol{\theta}_Y)$ can be directly computed using Eqs (32) and (33).
- Estimate the local SI $LS_{ij}(y,\boldsymbol{\theta}_\mathbf{X})$ with the aid of Eq. (22), based on the results of $f_Y(y,\boldsymbol{\theta}_\mathbf{X})$, $\mathbf{GS}_{ij}(\boldsymbol{\theta}_\mathbf{X})$ and $\mathbf{NT}(y,\boldsymbol{\theta}_Y)$.

As discussed above, the inputs for global sensitivity estimation are the moments of Y and $\partial\mathbf{E}/\partial\theta_{X_{ij}}$. The moments of Y are obtained through the dimensional reduction method described in section 5.1. The computation of $\partial\mathbf{E}/\partial\theta_{X_{ij}}$ is based on the evaluation points $\mathbf{x}_{pq}(r_p,r_q)$ and $\mathbf{x}_p(r_p)$ ($1\le p<q\le n$, r_p=1,...,l and r_q=1,..., l) and corresponding model outputs, all of which are byproducts of the distribution estimation process, as discussed in section 5.2. With these inputs readily obtained, the global SI can be computed. There is no additional model evaluation required in sensitivity estimation, thereby ensuring the efficiency of the method. With the moments of Y obtained, the TMNT can be constructed, and then the CDF/PDF of Y and local SI can be

readily obtained. In this sense, CDF/PDF and local SI can be treated as the byproducts of moment estimation and global SI, respectively.

6. Examples

6.1. Example 1: Weighted summation of two independent random variables

The first example considers a simple function as follows:

$$Y = h(\mathbf{X}) = k_1 X_1 + k_2 X_2, \tag{41}$$

where X_1 and X_2 are two independent random variables; and $k_1 = 2$ and $k_2 = -1$ are the coefficients.

To illustrate the procedure of the TSME method, detailed results are discussed for the case when X_1 and X_2 follow lognormal distributions with $\theta_{X_{11}} = 16$ and $\theta_{X_{21}} = 12$, respectively. Additionally, the coefficient of variance (COV) of X_1 and X_2 are assumed to be 0.05 and 0.10, respectively. Based on Fig. 2, the first step is to generate the evaluation points, which are transformed from $\hat{\mathbf{u}}$ and listed in Table 1. Then, the values of Y at the evaluation points can be readily

Table 1: Evaluation points in example 1

	r_q	r_p=1		r_p=2		r_p=3		r_p=4		r_p=5		r_p=6		r_p=7	
		X_1	X_2	X_1	X_2	X_1	X_2	X_1	X_2	X_1	X_2	X_1	X_2	X_1	X_2
	1	10.95	6.78	12.57	6.78	14.19	6.78	16	6.78	17.86	6.78	20.16	6.78	23.14	6.78
	2	10.95	8.34	12.57	8.34	14.19	8.34	16	8.34	17.86	8.34	20.16	8.34	23.14	8.34
	3	10.95	9.99	12.57	9.99	14.19	9.99	16	9.99	17.86	9.99	20.16	9.99	23.14	9.99
$\mathbf{x}_{12}(r_p, r_q)$	4	10.95	12	12.57	12	14.19	12	16	12	17.86	12	20.16	12	23.14	12
	5	10.95	14.10	12.57	14.10	14.19	14.10	16	14.10	17.86	14.10	20.16	14.10	23.14	14.10
	6	10.95	16.89	12.57	16.89	14.19	16.89	16	16.89	17.86	16.89	20.16	16.89	23.14	16.89
	7	10.95	20	12.57	20.76	14.19	20.76	16	20.76	17.86	20.76	20.16	20.76	23.14	20.76
$\mathbf{x}_1(r_p)$		10.95	12	12.57	9	14.19	12	16	12	17.86	12	20.16	12	23.14	12
$\mathbf{x}_2(r_p)$		16	6.78	16	8.34	16	9.99	16	12	16	14.10	16	16.89	16	20.76

computed. It can be observed from Table 1 that, there are some repeated values for $\mathbf{x}_p(r_p)$ and $\mathbf{x}_{pq}(r_p, r_q)$, and the number of model evaluations is 49 by eliminating the duplicated points. The next step is to evaluate the distribution of Y. First, with the aid of Eqs. (34) and (35), the first three moments about the origin of Y are computed as $\mathbf{E}$=(20, 413.48, 8816.02). Then, based on

Eqs. (4)-(6), the first three central moments of Y, i.e., $\boldsymbol{\theta}_Y$, can be transformed from $\mathbf{E}$ as (20, 3.6715, 0.1459). With $\boldsymbol{\theta}_Y$ obtained, the CDF and PDF of Y can be constructed based on the TMNT as given in Eqs. (18) and (30), respectively.

The third step is to conduct sensitivity estimation. First, the values of $g_{ijk}(\cdot,\cdot)$ are computed. The derivative of $f_{X_i}(X_i|\boldsymbol{\theta}_{X_i})$ with respect to $\boldsymbol{\theta}_{X_{ij}}$ is computed using finite difference method. Note that, as the lognormal distribution depends on two parameters, the sensitivity estimation focuses solely on the first two moments of $\mathbf{X}$. The values of $\partial\mathbf{E}/\partial\theta_{X_{ij}}$ are $\partial\mathbf{E}/\partial\theta_{X_{11}}$=$(2,\ 80,\ 2480.5)^T$, $\partial\mathbf{E}/\partial\theta_{X_{21}}$=$(-1,-40,-1240.2)^T$, $\partial\mathbf{E}/\partial\theta_{X_{12}}$=$(0,12.8,792.7)^T$, $\partial\mathbf{E}/\partial\theta_{X_{12}}$=$(0,3.6,210.1)^T$. Based on Eq. (14), $\partial\boldsymbol{\theta}_Y/\partial\mathbf{E}$ is

$$\frac{\partial\boldsymbol{\theta}_Y}{\partial\mathbf{E}}=\begin{pmatrix}1 & 0 & 0\\ -5.4473 & 0.1362 & 0\\ 24.0785 & -1.2285 & 0.0202\end{pmatrix}. \tag{42}$$

Substituting the values of $\partial\boldsymbol{\theta}_G/\partial\boldsymbol{E}_G(\boldsymbol{\theta})$ and $\partial\mathbf{E}/\partial\theta_{X_{ij}}$ into Eq. (13), the global sensitivity index $\mathbf{GS}_{ij}(\boldsymbol{\theta}_\mathbf{X})$ can be computed as $GS_{11}(\boldsymbol{\theta}_\mathbf{X})$=(2, 0, −0.0084), $GS_{21}(\boldsymbol{\theta}_\mathbf{X})$=(−1, 0, 0.0042), $GS_{12}(\boldsymbol{\theta}_\mathbf{X})$=(0, 1.7432, 0.2913), $GS_{22}(\boldsymbol{\theta}_\mathbf{X})$=(0, 0.4903, −0.1776). Based on Eqs. (32) and (33), $\mathbf{NT}(y,\boldsymbol{\theta}_Y)$ can be computed, and the local sensitivity index $LS_{ij}(y,\boldsymbol{\theta}_\mathbf{X})$ can then be obtained. For example, with y=10, $\mathbf{NT}(10,\boldsymbol{\theta}_Y)$=$(-1,2.7237,-4.8769)$, $LS_{11}(10,\boldsymbol{\theta}_\mathbf{X})=-0.0036$, $LS_{21}(10,\boldsymbol{\theta}_\mathbf{X})=0.0018$, $LS_{12}(10,\boldsymbol{\theta}_\mathbf{X})=0.0061$ and $LS_{22}(y,\boldsymbol{\theta}_\mathbf{X})=0.0040$.

To investigate the flexibility of the TMSE method for sensitivity estimation, several cases with varying statistical characteristics of X_1 and X_2 are considered, as listed in Table 2. All these distributions considered in this example are two-parametric, and the SE focuses on the first two moments of $\mathbf{X}$. Since the model for this example is relatively simple, it has analytical solution for the output distribution. For comparison, the global SI is also computed using analytical methods (details can be found in Appendix A.1), and the local SI is computed using finite difference method with the CDF of y analytically constructed (details can be found in Appendix A.2). The moments of y are compared in Table 3. As the mean and standard deviation of Y will not change with the distribution type of $\mathbf{X}$ for the case of the model considered in Eq. (41), the corresponding results are listed only for the case with $N_1 = 1$ for simplicity. It can be seen from Table 3 that, $\boldsymbol{\theta}_Y$ estimated using the point estimate method combined with BDRM is the same as the exact values, which illustrates the accuracy of the numerical methods. Furthermore, the distribution types of $\mathbf{X}$ will influence the skewness of Y. Representative PDFs and CDFs of Y for cases with

Table 2: Statistical information of random variables in example 1

Case		$N_D=1$		$N_D=2$		$N_D=3$		$N_D=4$		$N_D=5$		$N_D=6$	
		X_1 Norm.	X_2 Norm.	X_1 LogN.	X_2 LogN.	X_1 Norm.	X_2 Gamma	X_1 Norm.	X_2 Weibull	X_1 LogN.	X_2 Gamma	X_1 LogN.	X_2 Weibull
1	μ	16	9	16	9	16	9	16	9	16	9	16	9
	COV	0.05	0.10	0.05	0.10	0.05	0.10	0.05	0.10	0.05	0.10	0.05	0.10
2	μ	16	12	16	12	16	12	16	12	16	12	16	12
	COV	0.10	0.15	0.10	0.15	0.10	0.15	0.10	0.15	0.10	0.15	0.10	0.15
3	μ	16	15	16	15	16	15	16	15	16	15	16	15
	COV	0.15	0.20	0.15	0.20	0.15	0.20	0.15	0.20	0.15	0.20	0.15	0.20
4	μ	18	9	18	9	18	9	18	9	18	9	18	9
	COV	0.05	0.10	0.05	0.10	0.05	0.10	0.05	0.10	0.05	0.10	0.05	0.10
5	μ	18	12	18	12	18	12	18	12	18	12	18	12
	COV	0.10	0.15	0.10	0.15	0.10	0.15	0.10	0.15	0.10	0.15	0.10	0.15
6	μ	18	15	18	15	18	15	18	15	18	15	18	15
	COV	0.15	0.20	0.15	0.20	0.15	0.20	0.15	0.20	0.15	0.20	0.15	0.20
7	μ	20	9	20	9	20	9	20	9	20	9	20	9
	COV	0.05	0.10	0.05	0.10	0.05	0.10	0.05	0.10	0.05	0.10	0.05	0.10
8	μ	20	12	20	12	20	12	20	12	20	12	20	12
	COV	0.10	0.15	0.10	0.15	0.10	0.15	0.10	0.15	0.10	0.15	0.10	0.15
9	μ	20	15	20	15	20	15	20	15	20	15	20	15
	COV	0.15	0.20	0.15	0.20	0.15	0.20	0.15	0.20	0.15	0.20	0.15	0.20

N_D denotes the index of distribution combination; Norm. denotes Normal distribution; LogN. denotes Lognormal distribution; μ denotes the mean value.

$N_D = 2$ obtained analytically and using the TMNT as given in Eqs. (18) and (30) are compared in Figs. 3a-3f, which show that the reference and approximated CDF/PDF of Y are coincident with each other. This demonstrates the accuracy of the TMNT in conducting normal transformation for the considered cases. Furthermore, with different $\boldsymbol{\theta}_{\mathbf{X}}$, the CDF/PDF of Y shows significant differences, which demonstrates the necessary of conducting local sensitivity estimation.

The global SI, i.e., $\mathbf{GS}_{ij}(\boldsymbol{\theta}_{\mathbf{X}})$, obtained using analytical and the TMSE methods are compared in Table 4. For convenience, the global SIs for the kth central moments of Y with respect to $\theta_{X_{ij}}$ is denoted as GS_{ij}^k. Since two-parametric distributions are considered and in view of the model $h(\mathbf{X})$ considered in Eq. (41), GS_{ij}^1 and GS_{ij}^2 will not change with the distribution type, these values are listed once for all distribution types, while GS_{ij}^3 for different distribution types are listed separately. It can be seen from Table 4 that:

(1) For each case considered, GS_{1j}^l/GS_{2j}^l changes with l, which means the importance of X_i

Table 3: Central moments of model output in example 1

Case	Method	θ_{Y1}	θ_{Y2}	θ_{Y3}					
				N_D=1	N_D=2	N_D=3	N_D=4	N_D=5	N_D=6
1	Exact	23	1.836	0	0.0639	−0.0236	0.0843	0.0758	0.1837
	Approximate	23	1.836	0	0.0639	−0.0236	0.0843	0.0758	0.1837
2	Exact	20	3.672	0	0.1459	−0.0354	0.0622	0.1639	0.2615
	Approximate	20	3.672	0	0.1459	−0.0354	0.0622	0.1639	0.2615
3	Exact	17	5.660	0	0.1859	−0.0596	0.0524	0.2169	0.3289
	Approximate	17	5.660	0	0.1859	−0.0596	0.0524	0.2169	0.3288
4	Exact	27	2.012	0	0.0805	−0.0179	0.0640	0.0895	0.1714
	Approximate	27	2.012	0	0.0805	−0.0179	0.0640	0.0895	0.1714
5	Exact	24	4.025	0	0.1748	−0.0268	0.0472	0.1885	0.2626
	Approximate	24	4.025	0	0.1748	−0.0268	0.0472	0.1885	0.2626
6	Exact	21	6.177	0	0.2332	−0.0458	0.0403	0.2570	0.3432
	Approximate	21	6.177	0	0.2332	−0.0458	0.0403	0.2570	0.3431
7	Exact	31	2.193	0	0.0930	−0.0138	0.0494	0.1000	0.1633
	Approximate	31	2.193	0	0.0930	−0.0138	0.0494	0.1000	0.1633
8	Exact	28	4.386	0	0.1969	−0.0207	0.0365	0.2075	0.2647
	Approximate	28	4.386	0	0.1969	−0.0207	0.0365	0.2075	0.2647
9	Exact	25	6.708	0	0.2700	−0.0358	0.0315	0.2886	0.3559
	Approximate	25	6.708	0	0.2700	−0.0358	0.0315	0.2886	0.3559

on θ_{Yl} are different with different moments considered. This demonstrates the necessity of conducting SE with respect to distribution parameters of $\mathbf{X}$.

(2) Both GS_{ij}^1 and GS_{ij}^2 vary with $\boldsymbol{\theta}_{\mathbf{X}}$, while the distribution type of $\mathbf{X}$ has no effect on the values. This is a consequence of the considered model $h(\mathbf{X})$ in Eq. (41). In contrast, GS_{ij}^3 is significantly influenced by both $\boldsymbol{\theta}_{\mathbf{X}}$ and the distribution type of $\mathbf{X}$.

(3) GS_{ij}^1 and GS_{ij}^2 obtained from the TMSE method match the exact values, confirming the accuracy of the TMSE method. When analyzing the influence of $\boldsymbol{\theta}_{\mathbf{X}}$ on the skewness of Y, the results from both the TMSE and the exact methods are largely consistent, with only slight discrepancies in some cases. These differences arise because the TMSE method estimates $\boldsymbol{\theta}_Y$ based solely on $\boldsymbol{\theta}_{\mathbf{X}}$, whereas the exact method accounts for the entire distribution. Take the case with $\mathbf{X}$ follow normal distribution as an example, the skewness of Y should be 0 by definition and $\boldsymbol{\theta}_{\mathbf{X}}$ will has no influence on the skewness of Y. However, as the distribution type cannot be reflected by the moments considered here, the sensitivity of the skewness of Y with respect to $\boldsymbol{\theta}_{\mathbf{X}}$ is not zero obtained from the TMSE method as listed in Table 4.

The local SIs are computed by the TMSE and finite difference methods. For simplicity,

Table 4: Global sensitivity indices obtained from different methods in example 1

Case	i	j	GS^1_{ij}		GS^2_{ij}		GS^3_{i2}											
							$N_D = 1$		$N_D = 2$		$N_D = 3$		$N_D = 4$		$N_D = 5$		$N_D = 6$	
			Exact	TMSE	Exact	TMSE	Exact	TMSE	Exact	TMSE	Exact	TMSE	Exact	TMSE	Exact	TMSE	Exact	TMSE
1	1	1	2	2	0	0	0	0.033	−0.01	0.027	0	0.033	0	0.033	−0.01	0.027	−0.01	0.027
	2	1	−1	−1	0	0	0	0	0.004	0.003	0.003	0.001	0.005	0.012	0.003	0.001	0.005	0.013
	1	2	0	0	1.743	1.743	0	0	0.315	0.315	0.067	0.067	−0.24	−0.24	0.281	0.281	−0.03	−0.03
	2	2	0	0	0.490	0.490	0	0	−0.21	−0.21	−0.09	−0.09	0.163	0.159	−0.17	−0.17	0.083	0.079
2	1	1	2	2	0	0	0	0.004	−0.01	−0.01	0	0.004	0.000	0.004	−0.01	−0.01	−0.01	−0.01
	2	1	−1	−1	0	0	0	0	0.005	0.004	0.003	0.003	0.005	0.005	0.003	0.003	0.005	0.005
	1	2	0	0	1.743	1.743	0	0	0.291	0.291	0.050	0.050	−0.09	−0.89	0.266	0.266	0.127	0.127
	2	2	0	0	0.490	0.490	0	0	−0.18	−0.18	−0.06	−0.06	0.043	0.043	−0.14	−0.14	−0.04	−0.04
3	1	1	2	2	0	0	0	0.001	−0.02	−0.02	0	0.001	0.000	0.001	−0.02	−0.02	−0.02	−0.02
	2	1	−1	−1	0	0	0	0	0.006	0.006	0.004	0.004	0.007	0.007	0.004	0.004	0.007	0.007
	1	2	0	0	1.696	1.696	0	0	0.295	0.295	0.054	0.054	−0.05	−0.05	0.268	0.268	0.167	0.167
	2	2	0	0	0.530	0.530	0	0	−0.17	−0.17	−0.06	−0.06	0.004	0.004	−0.14	−0.14	−0.07	−0.07
4	1	1	2	2	0	0	0	0.032	−0.01	0.026	0.000	0.032	0.000	0.032	−0.01	0.026	−0.01	0.026
	2	1	−1	−1	0	0	0	0	0.003	0.002	0.002	0.001	0.004	0.014	0.002	0.001	0.004	0.014
	1	2	0	0	1.789	1.789	0	0	0.263	0.263	0.048	0.048	−0.17	−0.17	0.239	0.239	0.021	0.021
	2	2	0	0	0.447	0.447	0	0	−0.17	−0.17	−0.07	−0.07	0.132	0.128	−0.14	−0.14	0.060	0.056
5	1	1	2	2	0	0	0	0.004	−0.01	−0.01	0.000	0.004	0.000	0.004	−0.01	−0.01	−0.01	−0.01
	2	1	−1	−1	0	0	0	0	0.003	0.003	0.002	0.002	0.004	0.004	0.002	0.002	0.004	0.004
	1	2	0	0	1.789	1.789	0	0	0.246	0.246	0.036	0.036	−0.06	−0.06	0.228	0.228	0.129	0.129
	2	2	0	0	0.447	0.447	0	0	−0.15	−0.15	−0.05	−0.05	0.036	0.036	−0.12	−0.12	−0.04	−0.04
6	1	1	2	2	0	0	0	0.001	−0.02	−0.02	0	0.001	0	0.001	−0.02	−0.02	−0.01	−0.02
	2	1	−1	−1	0	0	0	0	0.005	0.005	0.003	0.003	0.005	0.005	0.003	0.003	0.005	0.005
	1	2	0	0	1.748	1.748	0	0	0.252	0.252	0.039	0.039	−0.03	−0.03	0.232	0.232	0.159	0.159
	2	2	0	0	0.486	0.486	0	0	−0.15	−0.15	−0.05	−0.05	0.005	0.005	−0.12	−0.12	−0.07	−0.07
7	1	1	2	2	0	0	0	0.030	−0.01	0.025	0	0.030	0.000	0.030	−0.01	0.025	−0.01	0.025
	2	1	−1	−1	0	0	0	0	0.002	0.002	0.002	0.001	0.003	0.015	0.002	0.001	0.003	0.015
	1	2	0	0	1.824	1.824	0	0	0.223	0.223	0.034	0.034	−0.12	−0.12	0.206	0.206	0.048	0.048
	2	2	0	0	0.410	0.410	0	0	−0.15	−0.15	−0.05	−0.05	0.107	0.102	−0.12	−0.12	0.043	0.038
8	1	1	2	2	0	0	0	0.004	−0.01	−0.01	0	0.004	0.000	0.004	−0.01	−0.01	−0.01	−0.01
	2	1	−1	−1	0	0	0	0	0.003	0.002	0.002	0.002	0.003	0.003	0.002	0.002	0.003	0.004
	1	2	0	0	1.824	1.824	0	0	0.212	0.212	0.026	0.026	−0.05	−0.05	0.198	0.198	0.127	0.127
	2	2	0	0	0.410	0.410	0	0	−0.13	−0.13	−0.04	−0.04	0.030	0.029	−0.10	−0.10	−0.03	−0.03
9	1	1	2	2	0	0	0	0.001	−0.02	−0.02	0	0.001	0	0.001	−0.02	−0.02	−0.02	−0.02
	2	1	−1	−1	0	0	0	0	0.004	0.004	0.002	0.002	0.004	0.004	0.002	0.002	0.004	0.004
	1	2	0	0	1.789	1.789	0	0	0.218	0.218	0.029	0.029	−0.03	−0.03	0.203	0.203	0.149	0.150
	2	2	0	0	0.447	0.447	0	0	−0.13	−0.13	−0.04	−0.04	0.005	0.005	−0.11	−0.11	−0.06	−0.06

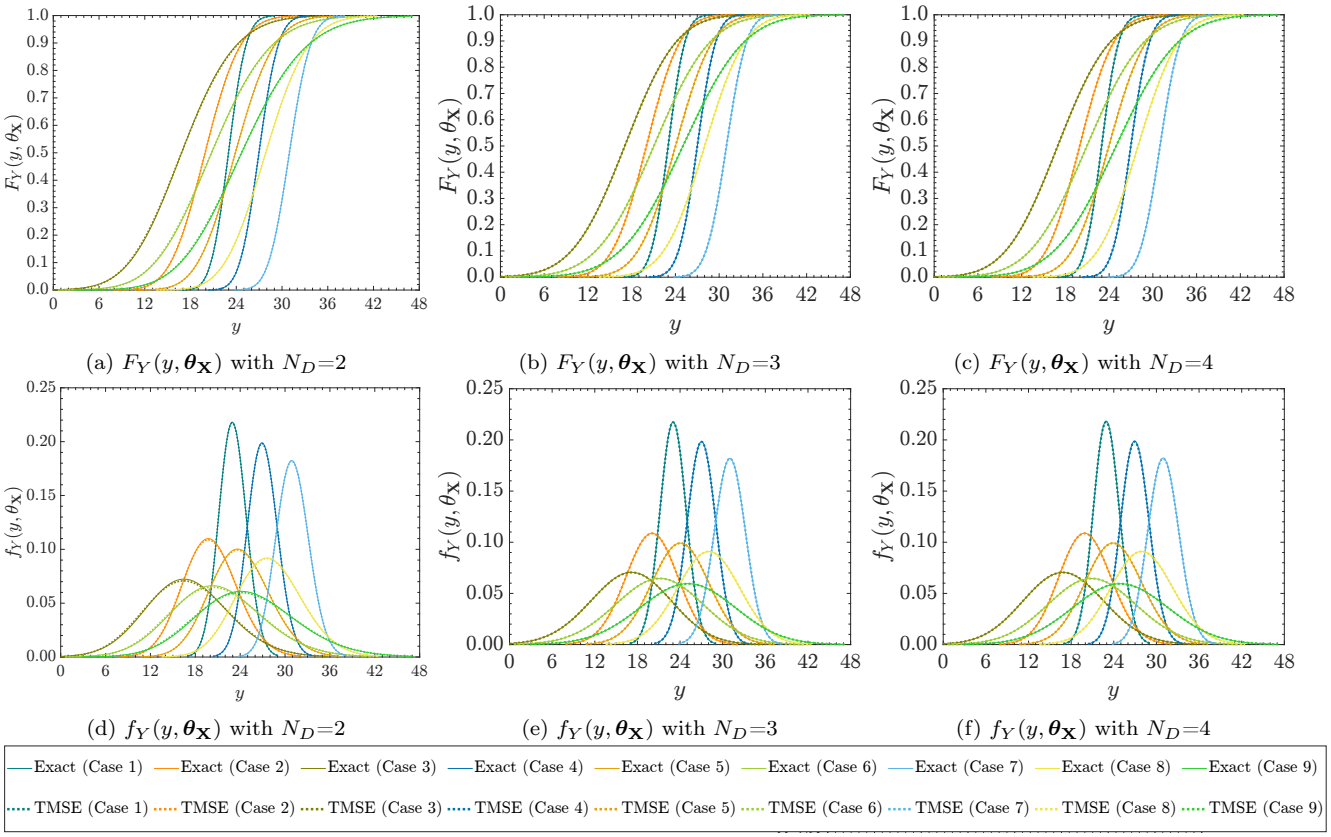

Figure 3: Representative $F_Y(y,\boldsymbol{\theta}_\mathbf{X})$ and $f_Y(y,\boldsymbol{\theta}_\mathbf{X})$ obtained from different methods in example 1

$LS_{11}(y,\boldsymbol{\theta}_\mathbf{X})$, $LS_{21}(y,\boldsymbol{\theta}_\mathbf{X})$, $LS_{12}(y,\boldsymbol{\theta}_\mathbf{X})$ and $LS_{22}(y,\boldsymbol{\theta}_\mathbf{X})$ for the case with N_D= 2 are compared in Figs. 4a-4e, while only $LS_{12}(y,\boldsymbol{\theta}_\mathbf{X})$ is plotted for the other cases in Figs. 4d-4i. It can be found that:

(1) $LS_{ij}(y,\boldsymbol{\theta}_\mathbf{X})$ is influenced by both $\boldsymbol{\theta}_\mathbf{X}$ and the distribution type, and varies non-monotonically with y. This highlights the necessity of conducting local sensitivity estimation for specific values of y, taking into account the distribution parameters of the input random variables. Notably, for two-parameter distributions, when the first two moments of $\mathbf{X}$ are fixed, the distribution type of $\mathbf{X}$ primarily affects the skewness and higher moments of Y. As a result, the influence of the distribution type of $\mathbf{X}$ is relatively small in this specific case.

(2) In all cases considered, $LS_{ij}(y,\boldsymbol{\theta}_\mathbf{X})$ obtained using the TMSE method closely align with the accurate values derived from the difference method based on the analytical $F_Y(y,\boldsymbol{\theta}_\mathbf{X})$, demonstrating the accuracy of the numerical approach developed for the TMSE method. Additionally, given the variety of distribution types in this example, the TMSE method exhibits considerable flexibility in estimating local sensitivity.

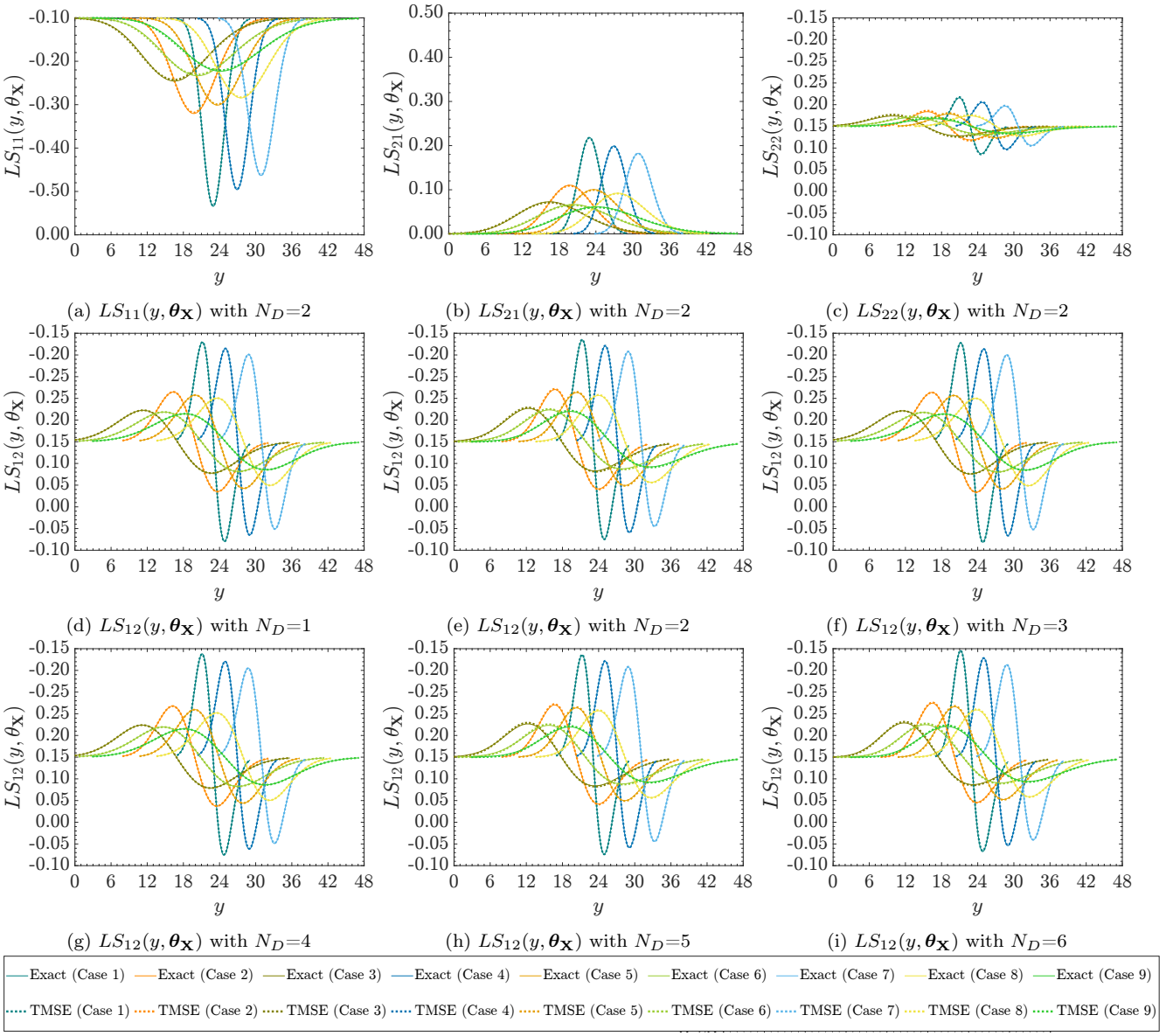

Figure 4: $LS_{ij}(y, \boldsymbol{\theta}_{\mathbf{X}})$ in example 1

6.2. Example 2: Safety factor of slope with multidimensional inputs

This example considers the safety factor of a slope as illustrated in Fig. 5, the simulator is adopted from Ref. [41] as follows:

$$Y = h(\mathbf{X}) = \frac{cA_s + N_s \tan\phi_s}{W(\sin\psi_p + \alpha\cos\psi_p) + V\cos\psi_p - T_s\sin\theta_s}, \tag{43}$$

$$A_s = (H - z)/\sin(\psi_p), \tag{44}$$

$$N_s = W(\cos\psi_p - \alpha\sin\psi_p) - U - V\sin\psi_p + T_s\cos\theta_s, \tag{45}$$

$$W = 0.5\gamma H^2\{[1 - (z/H)^2]\cot\psi_p - \cot\psi_f\}, \tag{46}$$

$$U = 0.5\gamma_W \cdot r \cdot z \cdot A_s, \quad V = 0.5\gamma_W \cdot r^2 \cdot z^2, \tag{47}$$

where $\gamma = 2.6 \times 10^4$ N/m^3; $\gamma_W = 1.0 \times 10^4$ N/m^3; $\psi_f = 50°$; $\psi_p = 35°$; $T_s = 0$; $\theta_s = 0$; $H =$ 60 m; and c and ϕ_s follow a bivariate lognormal distribution with a correlation coefficient of -0.5, while r, z, and α are mutually independent random variables. Their statistical characteristics are summarized in Table 5 For illustration, four cases with different COVs of $\mathbf{X}$ are considered.

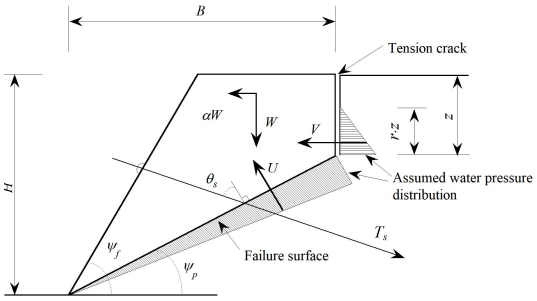

Figure 5: Illustration of slope for Example 2

Table 5: Statistical information of random variables in example 2

		c	ϕ_s	r	z	α
Distribution		Bivariate Lognormal		Weibull	Lognormal	Weibull
Mean		140 kPa	20°	0.3435	14 m^2	0.05496
COV	Case 1	0.20	0.08	0.765	0.214	0.765
	Case 2	0.22	0.10	0.841	0.236	0.841
	Case 3	0.24	0.12	0.917	0.257	0.917
	Case 4	0.26	0.14	0.994	0.279	0.994

With the model estimator known, SE can be performed using the TMSE method. The moment estimation in the TMSE method is carried out using the seven-point estimate method in combination with BDRM. The total number of samples required for BDRM with seven evaluation points is 391. Note that, the model considered in this example is strongly nonlinear, and thus BDRM cannot provide sufficient evaluation for SE considering the skewness of Y [33], and trivariate dimension reduction method (TDRM) is applied in computing $GS_{ij}^3(\boldsymbol{\theta}_{\mathbf{X}})$ (details can be found in Appendix C). The total number of samples required for TDRM with 7 evaluation points is 2551.

To investigate the influence of the number of evaluation points, BDRM and TDRM were also conducted with 9 and 11 evaluation points. The total numbers of model evaluations for BDRM and TDRM with 9 evaluation points are 681 and 5801, respectively, while those with 11 evaluation points are 1051 and 11051, respectively. For comparison, distribution estimation and sensitivity

analyses were also performed using Monte Carlo Simulation (MCS) with 10^8 samples (details are provided in Appendix B), serving as a benchmark for accuracy. The moments of Y obtained by the different methods are summarized in Table 6, where the numbers 7, 9, and 11 listed under the BDRM and TDRM columns indicate the number of evaluation points used for each method.

The PDF obtained by using the TMNT given in Eq. (30) is compared with the histogram obtained from MCS in Figs. 6a-6d. Figs. 6a-6d and Table 5 show that:

Table 6: Moments of model output in example 2

Case	Mean θ_{Y1}				Standard deviation θ_{Y2}				Skewness θ_{Y3}			
	MCS	BDRM			MCS	BDRM			MCS	TDRM		
		7	9	11		7	9	11		7	9	11
1	0.9315	0.9314	0.9314	0.9314	0.1155	0.1155	0.1155	0.1155	0.1729	0.1725	0.1726	0.1726
2	0.9321	0.9321	0.9321	0.9321	0.1266	0.1266	0.1266	0.1266	0.1598	0.1600	0.1601	0.1601
3	0.9329	0.9329	0.9329	0.9329	0.1379	0.1379	0.1379	0.1379	0.1488	0.1487	0.1488	0.1488
4	0.9338	0.9338	0.9338	0.9338	0.1495	0.1495	0.1495	0.1495	0.1378	0.1377	0.1378	0.1378

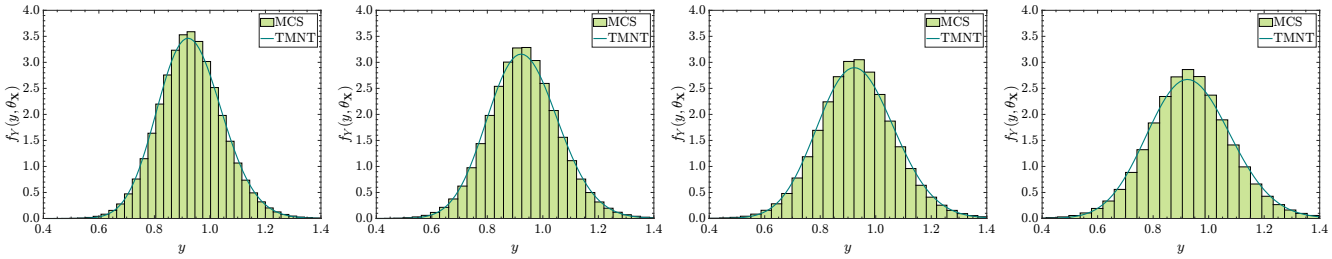

(a) Case 1 (b) Case 2 (c) Case 3 (d) Case 4

Figure 6: PDFs of model output in example 2

(1) The moments of Y computed by dimensional reduction methods are in close agreement with those from MCS, with the difference increases with the order of moments. This is because the higher moments are more difficult to obtain. The relative error of θ_{Y3} obtained from TDRM with 7 evaluation points is the largest (0.23%) for case 1.

(2) The moments of Y computed using different numbers of evaluation points show close agreement. Differences between results increase with higher-order moments and stronger non-Gaussianity. The largest relative difference occurs for the skewness in case 4 when comparing 7 and 11 evaluation points, amounting to 0.074%. This demonstrates that using 7 evaluation points provides sufficient accuracy. To balance accuracy and computational efficiency, seven evaluation points are recommended in the proposed method.

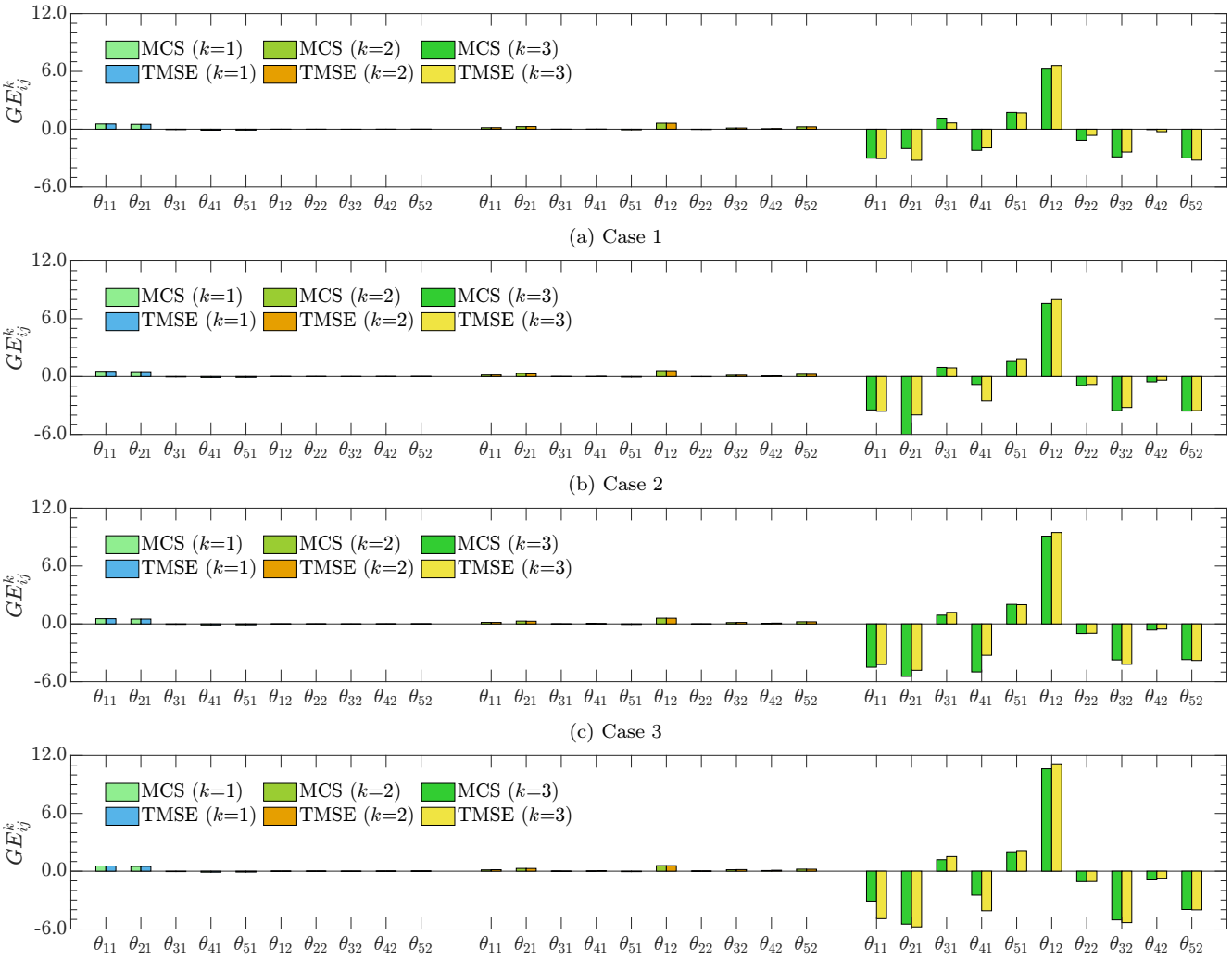

(a) Case 1

(b) Case 2

(c) Case 3

(d) Case 4

Figure 7: Global elasticity indexes (EIs) of model output in example 2

(3) The PDFs estimated using the TMNT-based model consistently align closely with those obtained from MCS, demonstrating the slightly error in $\boldsymbol{\theta}_Y$ obtained from SPEM-BDRM can be neglected in distribution estimation.

To eliminate the influence of units for different random variables, so-called elasticity definition is introduced [42], and the global and local elasticity indices are formulated as follows:

$$GE_{ij}^k = GS_{ij}^k \cdot \frac{\theta_{ij}}{\theta_{Yk}}, \tag{48}$$

$$LE_{ij}(y, \boldsymbol{\theta}_{\mathbf{X}}) = LS_{ij}(y, \boldsymbol{\theta}_{\mathbf{X}}) \cdot \theta_{ij}, \tag{49}$$

where GE_{ij}^k is the global elasticity index (EI) considering the kth central moments of Y; $LE_{ij}(y, \boldsymbol{\theta}_{\mathbf{X}})$ is the local EI. The global and local EIs obtained from the TMSE method are compared with those

from MCS in Figs. 7a-7d and 8a-8d, respectively. It can be found that:

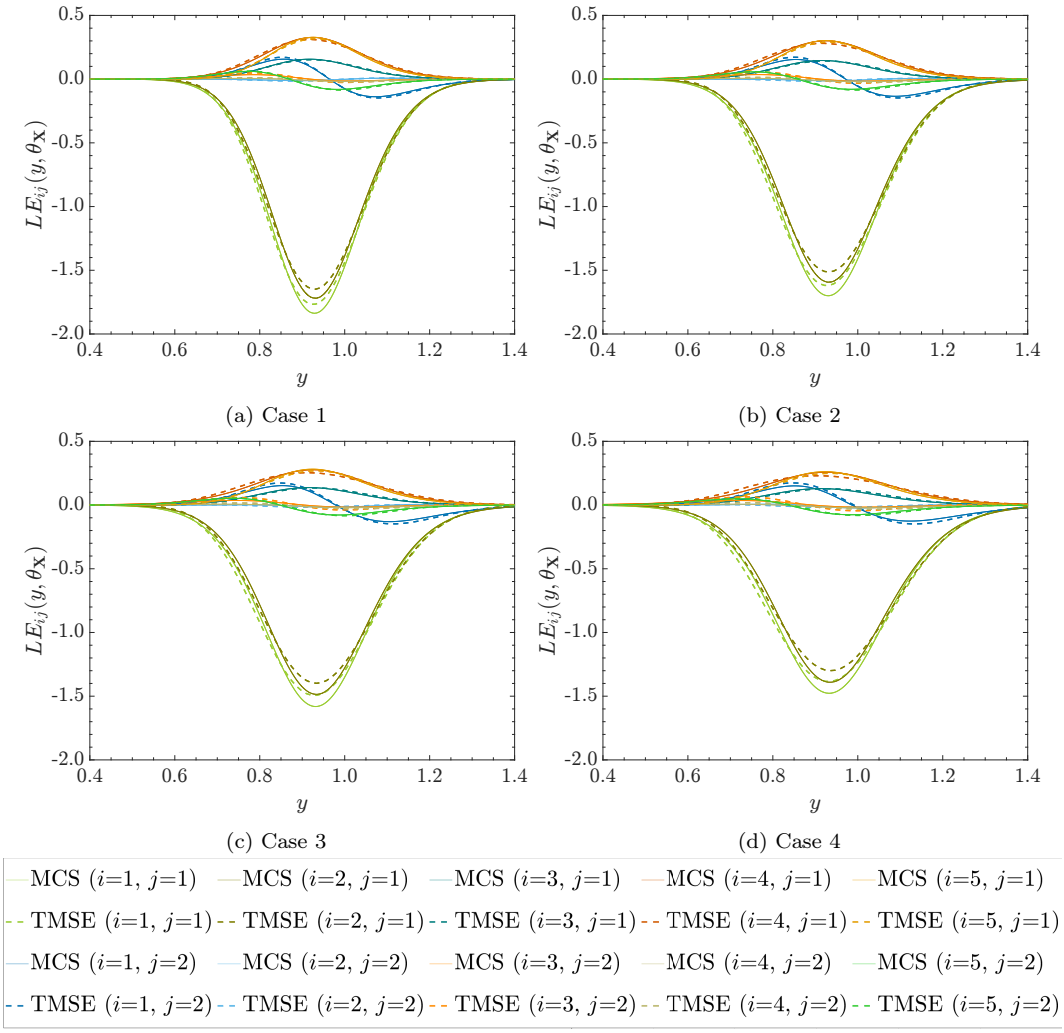

Figure 8: Local elasticity indexes (EIs) of model output in example 2

(1) The difference in GE_{ij}^k between TMSE and MCS results increases with the order k, primarily due to the increase of error in moment estimation. For $k = 1$ and 2, GE_{ij}^k obtained from the TMSE method closely matches that from MCS. As k increases, the discrepancy in GE_{ij}^k across methods grows, with the largest difference observed for GE_{22}^3. This proves the accuracy of the TMSE method for evaluating the global SI.

(2) The tendency of $LE_{ij}(y, \boldsymbol{\theta}_{\mathbf{X}})$ remains consistent across the cases considered. For a given random variable, i.e., fixed i, the absolute value of $LE_{i1}(y, \boldsymbol{\theta}_{\mathbf{X}})$ is consistently larger than that of $LE_{i2}(y, \boldsymbol{\theta}_{\mathbf{X}})$, indicating that the mean of $\mathbf{X}$ has a greater impact on the distribution of Y. The values of $LE_{ij}(y, \boldsymbol{\theta}_{\mathbf{X}})$ vary across cases. When the skewness of Y is relatively low, as in case 1, $LE_{ij}(y, \boldsymbol{\theta}_{\mathbf{X}})$ obtained from the TMSE method closely match those from

MCS. However, as the skewness of Y increases, so does the discrepancy between $LE_{ij}(y, \boldsymbol{\theta}_{\mathbf{X}})$ obtained from different methods. This difference is more pronounced compared to both the PDF and global EIs, as $LE_{ij}(y, \boldsymbol{\theta}_{\mathbf{X}})$ depends on the PDF, $\mathbf{GE}_{ij}$, and $\mathbf{NT}(y, \boldsymbol{\theta}_Y(\boldsymbol{\theta}_{\mathbf{X}}))$, as given in Eq. (22).

6.3. Example 3: Seepage problem below a dam computed using finite element method

The third example involves the study of a steady state confined seepage below a dam as shown in Fig. 9, which is adopted from Ref. [25]. The seepage discharge is investigated, which is computed

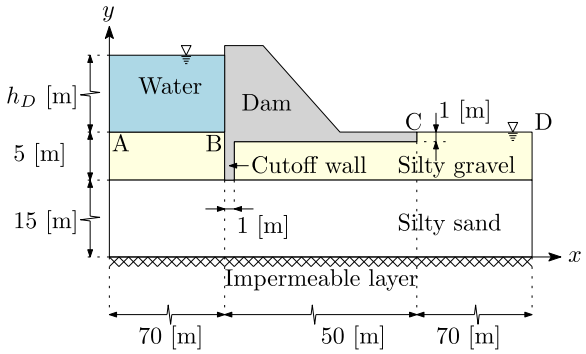

Figure 9: Schematic graph of the dam in example 3

in terms of an unit width of the dam and measured in units of volume over time and distance as follows:

$$Y = h(\mathbf{X}) = -\int_{\mathrm{CD}} k_{yy,2} \frac{\partial h_W}{\partial y} dx, \tag{50}$$

where CD represents the downstream side of the dam as shown in Fig 9; $k_{yy,2}$ is the vertical permeability of the second soil layer; and h_W is the hydraulic head, which is solved by the following differential equation:

$$k_{xx,i} \frac{\partial^2 h_W}{\partial x^2} + k_{yy,i} \frac{\partial^2 h_W}{\partial y^2} = 0, \quad i = 1, 2 \tag{51}$$

where $k_{xx,i}$ and $k_{yy,i}$ represent the horizontal and vertical permeabilities of the ith soil layer, respectively; and x and y denote horizontal and vertical coordinates, respectively. The boundary conditions for this equation are that: (1) h_W over segments AB and CD are 20+h_D m and 20 m, respectively, where $h_D = 5.0$ [m] is the height of water; (2) there is null flow over other boundaries. This equation is solved numerically applying the finite element (FE) method (see, e.g. Ref [43]), where the associated model comprises 3413 nodes and 1628 quadratic triangular elements. The permeabilities, i.e., $k_{xx,i}$ and $k_{yy,i}$ for $i = 1, 2$ are considered as random variables, with the statistical information summarized in Table 7.

Table 7: Statistical information of random variables in example 3 [25]

	Silty sand		Silty gravel	
	Horizontal $k_{xx,1}$	Vertical $k_{yy,1}$	Horizontal $k_{xx,2}$	Vertical $k_{yy,2}$
Distribution	Lognormal	Lognormal	Lognormal	Lognormal
Mean	5×10^{-7} [m/s]	2×10^{-7} [m/s]	5×10^{-6} [m/s]	2×10^{-6} [m/s]
COV	0.16	0.20	0.16	0.20

In this example, the seepage flow is challenging to characterize due to the geometry of the problem and the orthotropic properties of the soil permeability. The horizontal and vertical permeabilities of both the silty sand and silty gravel layers jointly influence the total seepage discharge, and changes in permeability values lead to variations in the flow paths across the soil domain. The governing differential equation, combined with heterogeneous boundary conditions, further contributes to the complexity of the solution, which is obtained numerically using the finite element method. When these permeabilities are modeled as random variables, their uncertainty propagates through the system, resulting in nontrivial output characteristics. These features make the problem representative for evaluating the proposed sensitivity estimation method.

The distribution estimation and SE are conducted using both the TMSE method and MCS with 10^6 samples. All scripts were implemented in MATLAB R2023b and executed on a computer equipped with a 13th Gen Intel(R) Core(TM) i7-1360P @ 2.20 GHz processor. In this example, the model $h(\mathbf{X})$ is implicit and incorporates a high-dimensional finite element (FE) model, resulting in an evaluation time of approximately 0.2 seconds per iteration. Consequently, the MCS becomes time-intensive, requiring about 1.325×10^5 seconds to complete, with parallelization employed to enhance computational efficiency.

To further investigate the impact of numerical methods on the performance of the TMSE method, the original moments of Y and its derivative with respect to θ_{ij} are approximated by point estimate method combining with both BDRM and TDRM, while the number of evaluation points n_E is set to be 7. The moments of Y calculated by various methods are summarized in Table 8, along with the corresponding number of model evaluations n_M required. Note that n_M needed for computing the moments of Y is identical to that required for both distribution estimation and sensitivity estimation. The PDF of Y modeled with the aid of the TMNT based on the moments of Y is compared with the histogram obtained from MCS in Fig. 10. It can be found that, there is slight difference in the moments of Y obtained by different methods, while the results of the TDRM is more accurate compared with those of the BDRM. Even though the

differences exist in moments of Y, the PDFs of Y obtained from different methods matches closely with the histogram obtained from MCS.

Table 8: Central moments of model outputs obtained from different methods in Example 3

	MCS	BDRM		TDRM	
		Value	R.E. (%)	Value	R.E. (%)
θ_{Y1} $(\times 10^{-6} L/h/m)$	1.7084	1.7084	0.0022	1.7084	0.0022
θ_{Y2} $(\times 10^{-7} L/h/m)$	1.6851	1.6850	0.0075	1.6850	0.0058
θ_{Y3}	0.2839	0.2795	1.5490	0.2811	0.9576
n_M	10^6	457	—	5641	—

R.E. denotes the relative error compared with the results of MCS.

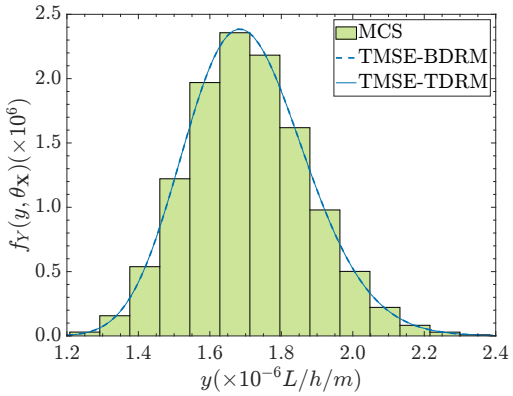

Figure 10: PDF of model output for example 3

The global SIs and EIs are compared in Figs. 11 and 12, respectively. Due to the limited number of samples in the MCS, which are insufficient for stable estimation of GS^3_{ij}, only the global SIs and EIs corresponding to the mean and standard deviation of Y are shown. It is evident that the results obtained using the TMSE method closely align with those from MCS. There is no significant difference in the results obtained using BDRM and TDRM for TMSE method. Notably, the sign of the global EI, GE^2_{32} derived from the TMSE method differs from that obtained through MCS. However, the sign of GS^2_{32} remains consistent across both methods. This discrepancy arises for global elasticities that have associated a small global sensitivity, which is an issue which has already been observed in a different context in [25]. However, the global sensitivities are estimated with small errors.

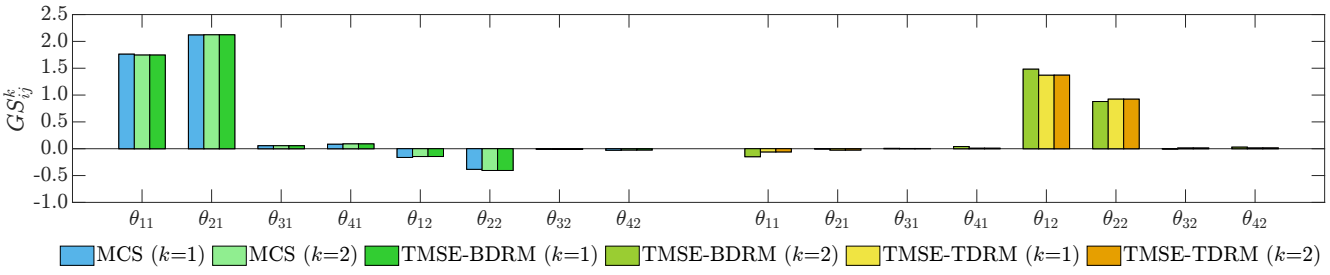

Figure 11: Global sensitivity indices from different methods for example 3

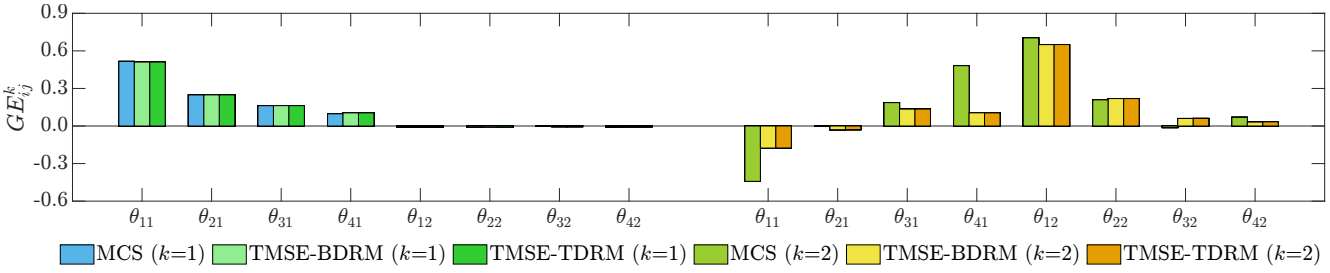

Figure 12: Global elastisity indices from different methods for example 3

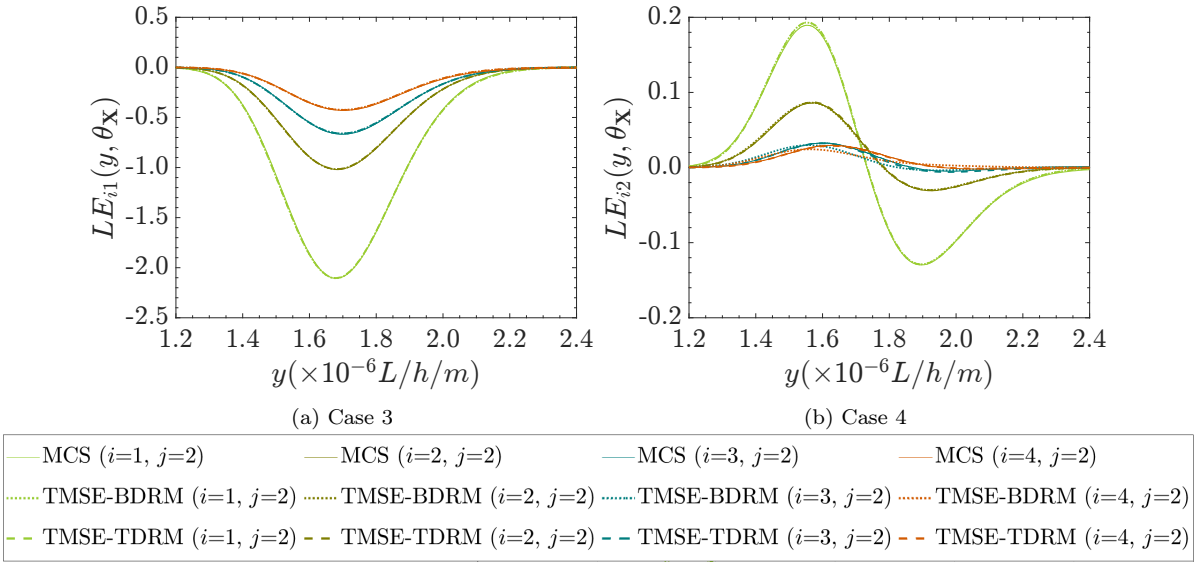

(a) Case 3 (b) Case 4

Figure 13: Local EIs of model output in example 3

The local EIs are compared in Figs. 13a and 13b. These figures demonstrate that the local EIs with respect to the mean values of the random variables, i.e., $LE_{i1}(y, \boldsymbol{\theta}_{\mathbf{X}})$, derived using the TMSE method are consistently in close agreement with those from MCS, for moments obtained through both BDRM and TDRM. When considering the standard deviation of the inputs, the local EIs $LE_{i2}(y, \boldsymbol{\theta}_{\mathbf{X}})$ obtained from the TMSE method using moments from TDRM also show good agreement with the MCS results. However, the TMSE method combined with BDRM shows slight deviations from the exact values. These deviations stem from errors in moment estimation, which are amplified through the normal transformation and affect the final sensitivity evaluation.

This suggests that, while BDRM provides sufficient accuracy for distribution and global sensitivity estimation, it may be less effective for assessing the sensitivity of the output CDF.

7. Discussion and Conclusions

The third moment normal transformation based sensitivity estimation (TMSE) method is introduced to estimate the sensitivity of model output stochastic properties with respect to input distribution parameters. This method defines two sensitivity indices (SIs): one that considers the first three moments and another focused on the cumulative failure probability. Practical approximation formulas for these SIs are developed with the aid of the TMNT, and a dimension reduction numerical approach is implemented to enhance computational efficiency. The method is demonstrated through three case studies, which include highly nonlinear models and computationally expensive FE models. Results indicate that different distribution parameters of input random variables exert significantly varied influences on the stochastic properties of model outputs. Thus, sensitivity estimation with respect to these distribution parameters is essential for a comprehensive understanding of model behavior. The numerical techniques developed for the TMSE method are both efficient and sufficiently accurate.

While the SIs defined in the TMSE method are theoretically robust for any problem, the numerical implementation has some constraints that pave the way for future research. The TMNT model, a pseudo-normal transformation technique based on the first three moments, provides reliable results when these moments adequately represent the output distribution. However, it fails to capture strong non-Gaussian behavior (the absolute skewness exceeds 2), heavy-tailed, bounded, multimodal, or mixture models. To enhance robustness, future work can explore the use of more flexible distribution models, such as the maximum entropy principle. The calculation of response moments via the dimensional reduction method discussed in Sections 5.1 and 5.2 implies quadratic scaling of computational cost with dimensionality and represents a challenge for large-scale applications. For high-dimensional problems, alternative moment estimation techniques, such as sampling-based methods or linear-moment-based approaches, may offer improved scalability at the expense of increased sampling effort, see e.g. Ref. [44]. A systematic comparison of these strategies is left for future work.

Acknowledgement

The study is partially supported by the Alexander von Humboldt Foundation for the postdoctoral grant of Xuan-Yi Zhang, and the Henriette Herz Scouting program (Matthias G.R. Faes). The authors gratefully acknowledge the supports.

Appendix A. Sensitivity estimation of weighted summation of independent random variables

Appendix A.1. Global sensitivity estimation

Consider a model defined as a weighted summation of n independent random variables $\mathbf{X}$, the first three moments of the model output Y can be analytically computed as follows:

$$\theta_{Y_1} = \mathbf{k}\boldsymbol{\theta}_{\mathbf{X}_1}, \tag{A.1}$$

$$\theta_{Y_2} = \sqrt{\mathbf{k}^{\circ 2}\boldsymbol{\theta}_{\mathbf{X}_2}^{\circ 2}}, \tag{A.2}$$

$$\theta_{Y_3} = \frac{\mathbf{k}^{\circ 3}(\boldsymbol{\theta}_{\mathbf{X}_3} \circ \boldsymbol{\theta}_{\mathbf{X}_2}^{\circ 3})}{\theta_{Y_2}^3}, \tag{A.3}$$

where $\mathbf{k}$ is a n-dimensional row vector of the weights for $\mathbf{X}$; $\boldsymbol{\theta}_{\mathbf{X}_i}$ is the n-dimensional column vectors of ith central moments of $\mathbf{X}$; $\circ$ denotes Hadamard product; and $(\cdot)^{\circ j}$ denotes the Hadamard power j of the argument. As $\boldsymbol{\theta}_Y$ can be explicitly computed from $\boldsymbol{\theta}_{\mathbf{X}}$ as given in Eqs. (A.1)-(A.3), the global SI can be directly obtained by taking the derivative of $\boldsymbol{\theta}_Y$ with respect to $\boldsymbol{\theta}_{\mathbf{X}}$. When $\mathbf{X}$ follows two-parametric distribution, $\partial\theta_{Y_i}/\partial\boldsymbol{\theta}_{\mathbf{X}_j}$ (i = 1, 2, 3 and j =1, 2) are formulated as follows:

$$\frac{\partial\theta_{Y_1}}{\partial\boldsymbol{\theta}_{\mathbf{X}_1}} = \mathbf{k}, \tag{A.4}$$

$$\frac{\partial\theta_{Y_2}}{\partial\boldsymbol{\theta}_{\mathbf{X}_2}} = \mathbf{k}^{\circ 2} \circ \frac{\boldsymbol{\theta}_{\mathbf{X}_2}}{\theta_{Y_2}}, \tag{A.5}$$

$$\frac{\partial\theta_{Y_3}}{\partial\boldsymbol{\theta}_{\mathbf{X}_1}} = \mathbf{k}^{\circ 3} \circ \frac{\boldsymbol{\theta}_{\mathbf{X}_2}^{\circ 3}}{\theta_{Y_2}^3} \circ \frac{\partial\boldsymbol{\theta}_{\mathbf{X}_3}}{\partial\boldsymbol{\theta}_{\mathbf{X}_1}}, \tag{A.6}$$

$$\frac{\partial\theta_{Y_3}}{\partial\boldsymbol{\theta}_{\mathbf{X}_2}} = \mathbf{k}^{\circ 3} \circ \frac{\boldsymbol{\theta}_{\mathbf{X}_2}^{\circ 2}}{\theta_{Y_2}^3} \circ \left(\boldsymbol{\theta}_{\mathbf{X}_2} \circ \frac{\partial\boldsymbol{\theta}_{\mathbf{X}_3}}{\partial\boldsymbol{\theta}_{\mathbf{X}_2}} + 3\boldsymbol{\theta}_{\mathbf{X}_3}\right) - \frac{3\theta_{Y_3}}{\theta_{Y_2}} \cdot \frac{\partial\theta_{Y_2}}{\partial\boldsymbol{\theta}_{\mathbf{X}_2}}. \tag{A.7}$$

For two-parameter distributions, $\partial\boldsymbol{\theta}_{\mathbf{X}_3}/\partial\boldsymbol{\theta}_{\mathbf{X}_j}$ is deterministic and can be obtained based on the specific formula of skewness of $\mathbf{X}$.

Appendix A.2. Local sensitivity estimation

To estimate the local SI, the key point is to construct the CDF of Y. For $h(\mathbf{X}) = \mathbf{kX}$, the inverse function of $h(\mathbf{X})$ with respect to X_i is monotonic, denoted as $h_i^{-1}(\mathbf{X}_{-i}, y)$, where $\mathbf{X}_i$ represents the random vector $\mathbf{X}$ with X_i excluded. Based on Eq. (2), when $h_i^{-1}(\mathbf{X}_{-i}, y)$ is monotonically increasing with y, $F_Y(y, \boldsymbol{\theta}_\mathbf{X})$ and $f_Y(y, \boldsymbol{\theta}_\mathbf{X})$ can be reformulated as follows:

$$\begin{aligned} F_Y(y, \boldsymbol{\theta}_\mathbf{X}) &= \int_{-\infty}^{+\infty} \cdots \int_{-\infty}^{+\infty} \left[\int_{-\infty}^{h_i^{-1}(\mathbf{x}_{-i}, y)} f_{X_i}(x_i, \boldsymbol{\theta}_{X_i})\, dx_i \right] f_{\mathbf{X}_{-i}}(\mathbf{x}_{-i}, \boldsymbol{\theta}_{\mathbf{X}_{-i}}) d\mathbf{x}_{-i} \qquad \text{(A.8)} \\ &= E\left\{ F_{X_i}\left[h_i^{-1}(\mathbf{x}_{-i}, y), \boldsymbol{\theta}_{X_i} \right] \right\}, \\ f_Y(y, \boldsymbol{\theta}_\mathbf{X}) &= \int_{-\infty}^{+\infty} \cdots \int_{-\infty}^{+\infty} \left[f_{X_i}(h_i^{-1}(\mathbf{x}_{-i}, y), \boldsymbol{\theta}_{X_i}) \frac{\partial h_i^{-1}(\mathbf{x}_{-i}, y)}{\partial y} \right] f_{\mathbf{X}_{-i}}(\mathbf{x}_{-i}, \boldsymbol{\theta}_{\mathbf{X}_{-i}}) d\mathbf{x}_{-i} \qquad \text{(A.9)} \\ &= E\left\{ f_{X_i}\left[h_i^{-1}(\mathbf{x}_{-i}, y)/k_i \right] \right\}, \end{aligned}$$

where k_i is the weight of X_i, which is positive for Eqs. (A.8) and (A.9). Similarly, when $h_i^{-1}(\mathbf{X}_{-i}, y)$ is monotonically decreasing with y, i.e., k_i is negative, $F_Y(y, \boldsymbol{\theta}_\mathbf{X})$ and $f_Y(y, \boldsymbol{\theta}_\mathbf{X})$ can be reformulated as follows

$$\begin{aligned} F_Y(y, \boldsymbol{\theta}_\mathbf{X}) &= \int_{-\infty}^{+\infty} \cdots \int_{-\infty}^{+\infty} \left[\int_{h_i^{-1}(\mathbf{x}_{-i}, y)}^{+\infty} f_{X_i}(x_i, \boldsymbol{\theta}_{X_i})\, dx_i \right] f_{\mathbf{X}_{-i}}(\mathbf{x}_{-i}, \boldsymbol{\theta}_{\mathbf{X}_{-i}}) d\mathbf{x}_{-i} \qquad \text{(A.10)} \\ &= 1 - E\left\{ F_{X_i}\left[h_i^{-1}(\mathbf{x}_{-i}, y), \boldsymbol{\theta}_{X_i} \right] \right\}, \\ f_Y(y, \boldsymbol{\theta}_\mathbf{X}) &= \int_{-\infty}^{+\infty} \cdots \int_{-\infty}^{+\infty} \left[1 - f_{X_i}(h_i^{-1}(\mathbf{x}_{-i}, y), \boldsymbol{\theta}_{X_i}) \frac{\partial h_i^{-1}(\mathbf{x}_{-i}, y)}{\partial y} \right] f_{\mathbf{X}_{-i}}(\mathbf{x}_{-i}, \boldsymbol{\theta}_{\mathbf{X}_{-i}}) d\mathbf{x}_{-i} \qquad \text{(A.11)} \\ &= 1 - E\left\{ f_{X_i}\left[h_i^{-1}(\mathbf{x}_{-i}, y)/k_i \right] \right\}. \end{aligned}$$

When there is only two random variables in $\mathbf{X}$ as investigated in example 1, the integrals required for constructing $F_Y(y, \boldsymbol{\theta}_\mathbf{X})$ and $f_Y(y, \boldsymbol{\theta}_\mathbf{X})$ are single dimensional, which can be easily computed. With $F_Y(y, \boldsymbol{\theta}_\mathbf{X})$ obtained, the local SI can be computed using the central difference method as follows:

$$LS_{ij}(y, \boldsymbol{\theta}_\mathbf{X}) = \frac{F_Y(y, \boldsymbol{\theta}_{\mathbf{X}^1}) - F_Y(y, \boldsymbol{\theta}_{\mathbf{X}^2})}{2\delta_{\theta_{X_{ij}}}} \qquad \text{(A.12)}$$

where $\delta_{\theta_{X_{ij}}}$ is a relatively small value with respect to $\theta_{X_{ij}}$; $\boldsymbol{\theta}_{\mathbf{X}^1}$ and $\boldsymbol{\theta}_{\mathbf{X}^2}$ are the moments of $\mathbf{X}$ with $\theta_{X_{ij}}$ set to be $\theta_{X_{ij}}+\delta_{\theta_{X_{ij}}}$ and $\theta_{X_{ij}}$-$\delta_{\theta_{X_{ij}}}$, respectively.

Appendix B. Sensitivity analysis using Monte Carlo Simulation

The definition of global SI given in Eq. (13) shows that, the key task for estimating global SI is to compute the derivative of original moments of Y with respect to θ_{ij}. Based on Eq. (16), such derivative can be approximated from samples as follows:

$$\frac{\partial E_k(\boldsymbol{\theta}_{\mathbf{X}})}{\partial \theta_{ij}} \cong \frac{1}{N_{mcs}} \sum_{l=1}^{N_{mcs}} g_{ijk}[\hat{\mathbf{x}}^{(l)}], \tag{B.1}$$

where N_{mcs} is the total number of samples generated; and $\hat{\mathbf{x}}^{(l)}$ is the lth sample generated. Substitute Eq. (B.1) into Eq. (13), the global SI can be readily obtained.

To estimate the local SI, CDF should be firstly estimated. Based on Eq. (2), the CDF of Y can be approximated from the samples as follows:

$$F_Y(\hat{y}^{(k)}, \boldsymbol{\theta}_{\mathbf{X}}) = \frac{1}{N_{mcs}} \sum_{l=1}^{N_{mcs}} I(\hat{\mathbf{x}}^{(l)}, \hat{y}^{(k)}) = \frac{\text{rank}(\hat{y}^{(k)} | \hat{\mathbf{y}}_{1:N_{mcs}})}{N_{mcs}}, \tag{B.2}$$

where $\hat{y}^{(k)}$ is the value of Y estimated as $h(\hat{\mathbf{x}}^{(k)})$; $\text{rank}(\hat{y}^{(k)})$ denotes the rank of $\hat{y}^{(k)}$ within the set $\hat{\mathbf{y}}_{1:N_{mcs}}$; and $\hat{\mathbf{y}}_{1:N_{mcs}}$ is the vector of all values of Y derived from the samples, sorted in ascending order. Combine Eqs. (9) and (B.2), local SI can be estimated using MCS as follows:

$$LS_{ij}(\hat{y}^{(k)}, \boldsymbol{\theta}_{\mathbf{X}}) = \frac{1}{N_{mcs}} \sum_{l=1}^{k} m_{ij}(\hat{x}_{i,rank}^{(l)}, \boldsymbol{\theta}_{X_i}) \tag{B.3}$$

where $\hat{x}_{i,rank}^{(l)}$ is the lth sample in the set of $\hat{\mathbf{x}}_{1:N_{mcs}}$; and $\hat{\mathbf{x}}_{1:N_{mcs}}$ is the vector of all samples of $\mathbf{X}$, sorted in ascending order based on the value of $h(\hat{\mathbf{x}}^{(k)})$

Appendix C. Moment estimation based on trivariate dimension reduction method

For strong nonlinear problem, where $G(\mathbf{X})$ shows significant nonlinearity in Gaussian space, the trivariate dimension reduction method (TDRM) [39] is advised to be applied. In the TDRM, the kth original moments of a performance function, i.e., $E_k(\boldsymbol{\theta})$, is approximated by a summation

of some one-, two- and three-dimensional functions as follows:

$$E_k(\boldsymbol{\theta}) \cong \sum_{m=1}^{n-2}\sum_{l>m}^{n-1}\sum_{s>l}^{n} E_{mls}^k(\boldsymbol{\theta}) - (n-3)\sum_{m=1}^{n-1}\sum_{l>m}^{n} E_{ml}^k(\boldsymbol{\theta}) + \frac{(n-3)(n-2)}{2}\sum_{m=1}^{n} E_m^k(\boldsymbol{\theta}) - \frac{(n-3)(n-2)(n-1)}{6}[G(\boldsymbol{\mu})]^k, \tag{C.1}$$

$$E_{mls}^k(\boldsymbol{\theta}) = \sum_{r_m=1}^{q}\sum_{r_l=1}^{q}\sum_{r_s=1}^{q} P_{r_m}P_{r_l}P_{r_s}[G(\mu_1,\cdots,\hat{x}_m(r_m|\boldsymbol{\theta}),\cdots,\hat{x}_l(r_l|\boldsymbol{\theta}),\cdots,\hat{x}_s(r_s|\boldsymbol{\theta}),\cdots,\mu_n)]^k, \tag{C.2}$$

$$E_{ml}^k(\boldsymbol{\theta}) = \sum_{r_m=1}^{q}\sum_{r_l=1}^{q} P_{r_m}P_{r_l}[G(\mu_1,\cdots,\hat{x}_m(r_m|\boldsymbol{\theta}),\cdots,\hat{x}_l(r_l|\boldsymbol{\theta}),\cdots,\mu_n)]^k, \tag{C.3}$$

$$E_m^k(\boldsymbol{\theta}) = \sum_{r_m=1}^{q} P_{r_m}[G(\mu_1,\cdots,\hat{x}_m(r_m|\boldsymbol{\theta}),\cdots,\mu_n)]^k, \tag{C.4}$$

where P_{r_s} is the weight of the r_sth evaluation point. Based on the TDRM, $\partial E_k(\boldsymbol{\theta})/\partial\theta_{ij}$ defined in Eq. (16) can be calculated as follows:

$$\frac{\partial E_k(\boldsymbol{\theta})}{\partial\theta_{ij}} \cong \sum_{m=1}^{n-2}\sum_{l>m}^{n-1}\sum_{s>l}^{n} D_{mls}(\boldsymbol{\theta}) - (n-3)\sum_{m=1}^{n-1}\sum_{l>m}^{n} D_{ml}(\boldsymbol{\theta}) + \frac{(n-3)(n-2)}{2}\sum_{m=1}^{n} D_m(\boldsymbol{\theta}) - \frac{(n-3)(n-2)(n-1)}{6} g_{ijk}(\boldsymbol{\mu}), \tag{C.5}$$

$$D_{mls}(\boldsymbol{\theta}) = \sum_{r_m=1}^{q}\sum_{r_l=1}^{q}\sum_{r_s=1}^{q} P_{r_m}P_{r_l}P_{r_s} g_{ijk}[\mu_1,\cdots,\hat{x}_m(r_m|\boldsymbol{\theta}),\cdots,\hat{x}_l(r_l|\boldsymbol{\theta}),\cdots,\hat{x}_s(r_s|\boldsymbol{\theta}),\cdots,\mu_n], \tag{C.6}$$

$$D_{ml}(\boldsymbol{\theta}) = \sum_{r_m=1}^{q}\sum_{r_l=1}^{q} P_{r_m}P_{r_l} g_{ijk}[\mu_1,\cdots,\hat{x}_m(r_m|\boldsymbol{\theta}),\cdots,\hat{x}_l(r_l|\boldsymbol{\theta}),\cdots,\mu_n], \tag{C.7}$$

$$D_m(\boldsymbol{\theta}) = \sum_{r_m=1}^{q} P_{r_m} g_{ijk}[\mu_1,\cdots,\hat{x}_m(r_m|\boldsymbol{\theta}),\cdots,\mu_n]. \tag{C.8}$$

References

[1] S. Razavi, A. Jakeman, A. Saltelli, C. Prieur, B. Iooss, E. Borgonovo, E. Plischke, S. L. Piano, T. Iwanaga, W. Becker, et al., The future of sensitivity analysis: an essential discipline for systems modeling and policy support, Environmental Modelling & Software 137 (2021) 104954.

[2] I. Sobol', Sensitivity estimates for nonlinear mathematical models, Math. Model. Comput. Exp. 1 (1993) 407.

[3] Z. Wan, S. Wang, Z. Wu, X. Wang, Dimension-independent single-loop Monte Carlo simulation method for estimate of Sobol' indices in variance-based sensitivity analysis, Reliability Engineering & System Safety 263 (2025) 111236.

[4] I. Papaioannou, D. Straub, Variance-based reliability sensitivity analysis and the form α-factors, Reliability Engineering & System Safety 210 (2021) 107496.

[5] I. Papaioannou, D. Straub, FORM-based global reliability sensitivity analysis of systems with multiple failure modes, Reliability Engineering & System Safety 260 (2025) 110974.

[6] X. Guan, The moment quadrature method for global sensitivity analysis, Reliability Engineering & System Safety 265 (PartA) (2026) 111460.

[7] W. Becker, Metafunctions for benchmarking in sensitivity analysis, Reliability Engineering & System Safety 204 (2020) 107189.

[8] B. Sudret, Global sensitivity analysis using polynomial chaos expansions, Reliability Engineering & System Safety 93 (7) (2008) 964–979.

[9] T. A. Mara, W. E. Becker, Polynomial chaos expansion for sensitivity analysis of model output with dependent inputs, Reliability Engineering & System Safety 214 (2021) 107795.

[10] X. Shang, L. Wang, H. Fang, L. Lu, Z. Zhang, Active learning of ensemble polynomial chaos expansion method for global sensitivity analysis, Reliability Engineering & System Safety 249 (2024) 110226.

[11] K. Cheng, Z. Lu, C. Ling, S. Zhou, Surrogate-assisted global sensitivity analysis: an overview, Structural and Multidisciplinary Optimization 61 (2020) 1187–1213.

[12] Q. Shao, A. Younes, M. Fahs, T. A. Mara, Bayesian sparse polynomial chaos expansion for global sensitivity analysis, Computer Methods in Applied Mechanics and Engineering 318 (2017) 474–496.

[13] Y. Shang, M. Nogal, R. Teixeira, A. R. M. Wolfert, Extreme-oriented sensitivity analysis using sparse polynomial chaos expansion. application to train–track–bridge systems, Reliability Engineering & System Safety 243 (2024) 109818.

[14] X. Wu, Z. Lu, Efficient global reliability sensitivity method by combining dimensional reduction integral with stochastic collocation, Reliability Engineering & System Safety 260 (2025) 110993.

[15] A. Dell'Oca, M. Riva, A. Guadagnini, Moment-based metrics for global sensitivity analysis of hydrological systems, Hydrology and Earth System Sciences 21 (12) (2017) 6219–6234.

[16] E. Borgonovo, A new uncertainty importance measure, Reliability Engineering & System Safety 92 (6) (2007) 771–784.

[17] F. Pianosi, T. Wagener, Distribution-based sensitivity analysis from a generic input-output sample, Environmental Modelling & Software 108 (2018) 197–207.

[18] W. Yun, Z. Lu, X. Jiang, An efficient method for moment-independent global sensitivity analysis by dimensional reduction technique and principle of maximum entropy, Reliability Engineering & System Safety 187 (2019) 174–182.

[19] P. P. Li, Y. G. Zhao, C. Dang, M. Broggi, M. A. Valdebenito, M. G. Faes, An efficient bayesian updating framework for characterizing the posterior failure probability, Mechanical Systems and Signal Processing 222 (2025) 111768.

[20] M. A. Valdebenito, X. Yuan, M. G. Faes, Augmented first-order reliability method for estimating fuzzy failure probabilities, Structural Safety 105 (2023) 102380.

[21] P. Bjerager, S. Krenk, Parametric sensitivity in first order reliability theory, Journal of Engineering Mechanics 115 (7) (1989) 1577–1582.

[22] I. Enevoldsen, J. D. Sørensen, Reliability-based optimization of series systems of parallel systems, Journal of Structural Engineering 119 (4) (1993) 1069–1084.
[23] N. Metropolis, S. Ulam, The Monte Carlo method, Journal of the American statistical association 44 (247) (1949) 335–341.
[24] R. Melchers, Importance sampling in structural systems, Structural Safety 6 (1) (1989) 3–10.
[25] M. A. Valdebenito, H. A. Jensen, H. Hernández, L. Mehrez, Sensitivity estimation of failure probability applying line sampling, Reliability Engineering & System Safety 171 (2018) 99–111.
[26] S.-K. Au, J. L. Beck, Estimation of small failure probabilities in high dimensions by subset simulation, Probabilistic Engineering Mechanics 16 (4) (2001) 263–277.
[27] S.-K. Au, E. Patelli, Rare event simulation in finite-infinite dimensional space, Reliability Engineering & System Safety 148 (2016) 67–77.
[28] V. Dubourg, B. Sudret, Meta-model-based importance sampling for reliability sensitivity analysis, Structural Safety 49 (2014) 27–36.
[29] L. G. Zhang, Z. Z. Lu, L. Cheng, Z. C. Tang, Emulator model–based analytical solution for reliability sensitivity analysis, Journal of Engineering Mechanics 141 (8) (2015) 04015016.
[30] D. W. Jia, Z. Y. Wu, An improved adaptive kriging model for importance sampling reliability and reliability global sensitivity analysis, Structural Safety 107 (2024) 102427.
[31] Y. G. Zhao, T. Ono, Moment methods for structural reliability, Structural Safety 23 (1) (2001) 47–75.
[32] Z. Z. Lu, J. Song, S. F. Song, Z. F. Yue, J. Wang, Reliability sensitivity by method of moments, Applied Mathematical Modelling 34 (10) (2010) 2860–2871.
[33] X. Y. Zhang, M. A. Valdebenito, Y. G. Zhao, M. G. Faes, Probability sensitivity estimation with respect to distribution parameters via the method of moments, ASCE-ASME Journal of Risk and Uncertainty in Engineering Systems, Part A: Civil Engineering 11 (4) (2025) 04025081.
[34] M. G. Faes, M. Daub, S. Marelli, E. Patelli, M. Beer, Engineering analysis with probability boxes: A review on computational methods, Structural Safety 93 (2021) 102092.
[35] Y. G. Zhao, Z. H. Lu, Structural reliability: approaches from perspectives of statistical moments, John Wiley & Sons, 2021.
[36] Y. G. Zhao, T. Ono, Third-moment standardization for structural reliability analysis, Journal of Structural Engineering 126 (2000) 724–732. doi:10.1061/(ASCE)0733-9445(2000)126:6(724).
[37] Q. Qin, X. Y. Zhang, Z. H. Lu, Y. G. Zhao, Simplified third-order normal transformation and its application in structural reliability analysis, Engineering Mechanics 37 (12) (2020) 78–86, 113. doi:10.6052/j.issn.1000-4750.2020.01.0015 (in Chinese).
[38] Y. G. Zhao, T. Ono, New point estimates for probability moments, Journal of Engineering Mechanics 126 (4) (2000) 433–436.
[39] H. Xu, S. Rahman, A generalized dimension-reduction method for multidimensional integration in stochastic mechanics, International Journal for Numerical Methods in Engineering 61 (12) (2004) 1992–2019.
[40] M. Hohenbichler, R. Rackwitz, Non-normal dependent vectors in structural safety, Journal of the Engineering Mechanics Division 107 (6) (1981) 1227–1238.
[41] Z. H. Lu, C. H. Cai, Y. G. Zhao, Structural reliability analysis including correlated random variables based on third-moment transformation, Journal of Structural Engineering 143 (8)

(2017) 04017067.
[42] M. Lemaire, Structural reliability, John Wiley & Sons, 2013.
[43] K. J. Bathe, Finite element procedures, Klaus-Jurgen Bathe, 2006.
[44] C. H. Acevedo, M. A. Valdebenito, I. V. González, H. A. Jensen, M. G. Faes, Variance-reduced estimation of third-order statistics using control variates with splitting, Reliability Engineering & System Safety 267 (2026) 111859.